AD-A107 587 SYSTEMS SCIENCE AND SOFTWARE LA JOLLA CA F/G 17/10
DETECTION, LOCATION AND IDENTIFICATION OF EXPLOSIONS AND EARTHQ--ETC(U)
JUN 81 J R MURPHY
UNCLASSIFIED SSS-R-81-5010 NL

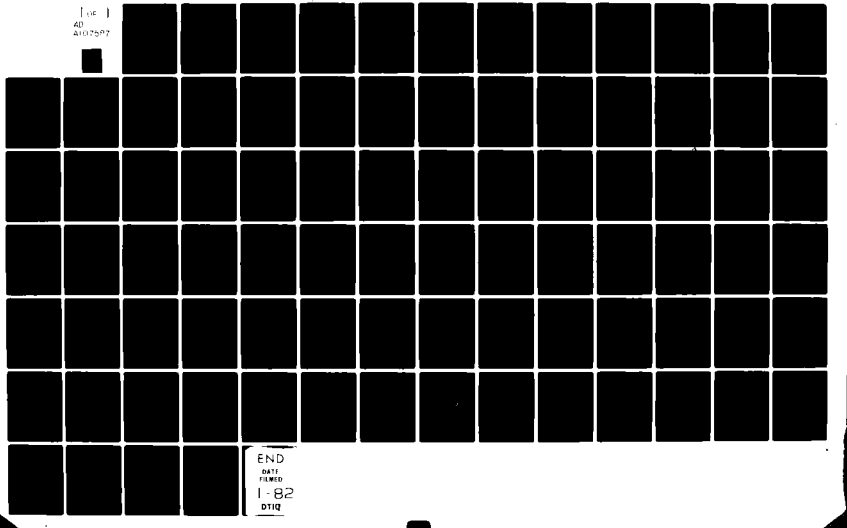

END
DATE FILMED
1-82
DTIC

JUNE 1981

(9)

DETECTION, LOCATION AND IDENTIFICATION OF EXPLOSIONS AND EARTHQUAKES USING REGIONAL SEISMIC DATA RECORDED AT A SINGLE STATION

ACOMC107

PREPARED FOR

U.S. ARMS CONTROL AND DISARMAMENT AGENCY

PREPARED BY

SYSTEMS, SCIENCE AND SOFTWARE
P.O. BOX 1620
LA JOLLA, CALIFORNIA 92038

DISCLAIMER NOTICE

THIS DOCUMENT IS BEST QUALITY PRACTICABLE. THE COPY FURNISHED TO DTIC CONTAINED A SIGNIFICANT NUMBER OF PAGES WHICH DO NOT REPRODUCE LEGIBLY.

AD-A107587

50272-101

REPORT DOCUMENTATION PAGE	1. REPORT NO.	2.	3. Recipient's Accession No.
4. Title and Subtitle: DETECTION, LOCATION AND IDENTIFICATION OF EXPLOSIONS AND EARTHQUAKES USING REGIONAL SEISMIC DATA RECORDED AT A SINGLE STATION			5. Report Date: Approved July, 1981 6.
7. Author(s): J. R. Murphy			8. Performing Organization Rept. No.: SSS-R-81-5010
9. Performing Organization Name and Address: SYSTEMS, SCIENCE AND SOFTWARE P.O. Box 1620 La Jolla, California 92038			10. Project/Task/Work Unit No. 11. Contract(C) or Grant(G) No. (C) AC0MC107 (G)
12. Sponsoring Organization Name and Address: United States Arms Control and Disarmament Agency Washington, D.C. 20451			13. Type of Report & Period Covered: Final Report Aug. 1980-Aug. 1981 14.

15. Supplementary Notes

16. Abstract (Limit: 200 words)

This report summarizes the results of an analysis of the various factors affecting the detection, location and event identification capability of a single seismic station in the regional distance range. A regional seismic detection model is described in Section II where it is applied to the evaluation of the frequency dependent detectability of underground explosions in various source media. On the basis of these analyses it is concluded that P waves from explosions with yields as small as 1 kt should be detectable at ranges on the order of 1000 km or more over regional propagation paths characteristic of the Eastern U.S. Event location capability associated with single station seismic data is assessed in Section III where it is concluded that epicentral distance accuracies on the order of 10 to 15 km and source azimuth accuracies of better than 10 degrees are achievable using routinely available data processing procedures. Single station, regional event discrimination capability is reviewed in Section IV where it is concluded that, although questions remain concerning the reliability of simple regional phase amplitude ratio discriminants (e.g. L_g/P), available evidence suggests that regional versions of the M_s/m_b and short-period P wave spectral discriminants generally provide good event separation when applied to single station data.

17. Document Analysis a. Descriptors

SEISMIC
DETECTION
LOCATION
IDENTIFICATION
EXPLOSION
NUCLEAR
REGIONAL

b. Identifiers/Open-Ended Terms

c. COSATI Field/Group: Seismology

18. Availability Statement: Release Unlimited	19. Security Class (This Report): Unclassified	21. No. of Pages: 84
	20. Security Class (This Page): Unclassified	22. Price

TABLE OF CONTENTS

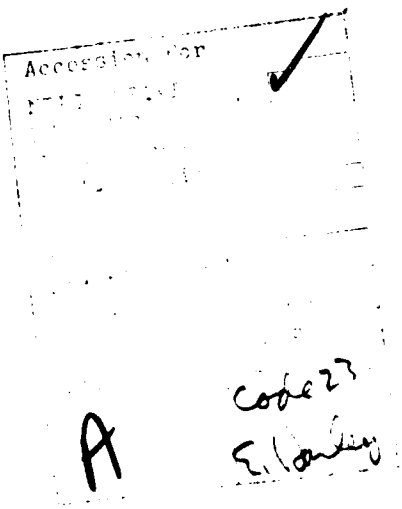

LIST OF ILLUSTRATIONS

LIST OF ILLUSTRATIONS (Continued)

LIST OF ILLUSTRATIONS (Continued)

LIST OF ILLUSTRATIONS (Continued)

EXECUTIVE SUMMARY

This report summarizes the results of an analysis of the various factors affecting the detection, location and identification capability of a single seismic station in the regional distance range. The primary objective of this study has been to extend previous teleseismic analyses of network performance to include a consideration of the potential advantages associated with the analyses of broadband seismic data of the type which would be expected to be recorded by in-country stations deployed for treaty monitoring purposes.

A regional seismic detection model is described in Section II where it is applied to the evaluation of the frequency-dependent detectability of fully coupled underground explosions in a variety of geologic environments. This model includes a source description which predicts that the seismic coupling of explosions in wet tuff/rhyolite, granite and shale source environments will be quite similar, but that explosions in salt will couple significantly better and explosions in dry alluvium/tuff significantly less well than those in the other three media. Various simulations are performed with this model and used to assess the dependence of detection thresholds on variables such as frequency, the yield of the explosion and the source medium. On the basis of these simulations, it is concluded that even 1 kt explosions in low coupling media such as dry alluvium/tuff should be detectable at ranges exceeding 2000 km for regional propagation paths similar to those of the Eastern U.S. Furthermore, evidence is presented which suggests that the frequency components of the signal which will define these limits of detectability for explosions with yields of about 1 kt lie in the 2-3 Hz range. Thus, it is concluded that the availability of broadband data is of less significance with regard to the detection of fully coupled explosions than in the previously considered detection of

decoupled explosions (Murphy, 1980).

The location of seismic events using data recorded at only a single station is discussed in Section III where observed regional interphase arrival times are used to estimate epicentral distances and three-component, particle motion data are used to constrain the azimuth of the source. Simulation experiments are conducted using measured regional arrival time data from U.S. and Russian earthquakes and explosions and, on the basis of these preliminary studies, it is suggested that epicentral distance can generally be estimated to within 10 to 15 km using data recorded at a calibrated station at which multiple regional phases are well recorded. The corresponding accuracy in source azimuth determination from single station data is estimated to be on the order of 10 degrees. Consequently, the evidence suggests that at epicentral distances on the order of 1000 km, the component of the location error due to uncertainty in source azimuth is currently an order of magnitude larger than that due to uncertainty in epicentral distance.

Single station event discrimination capability is reviewed in Section IV with particular emphasis on the applicability of the L_g/P, M_s/m_b and short-period P wave spectral discriminants to the classification of regional seismic data. On the basis of this analysis, it is concluded that while questions remain concerning the general applicability of the simple L_g/P amplitude ratio discriminant, there are some preliminary indications that an L_g/P spectral ratio discriminant may provide for more consistent event separation. A regional version of M_s/m_b based on the ratio of the P_n amplitude to the amplitude of the Rayleigh wave at periods near 12 seconds is shown to provide good separation between Nevada Test Site explosions and earthquakes and it is concluded that it may be useful in a single station context. Finally, preliminary spectral analyses of regional P wave data recorded from Russian

explosions and earthquakes are presented which suggest that the single station, short-period P wave spectral discriminant may be even more effective against such broadband data than it is against teleseismic data from the same events.

I. INTRODUCTION

In order to effectively monitor any eventual Comprehensive Test Ban Treaty (CTBT) using seismic means, it will be necessary to have the capability to detect, locate and identify all seismic activity down to very low magnitudes. In general, it is considered to be necessary to detect at three or more stations in order to locate an event and many of the conventional discriminants (e.g. M_s/m_b, long period S, etc.) require data from several widely spaced stations in order to suppress the large uncertainty introduced by the seismic radiation patterns (i.e. azimuthal dependence) associated with the various waves of interest. However, for small events near the detection threshold, it is possible that at least some of the seismic phases of interest might be detected at only a single in-country station, particularly in cases in which evasion is attempted. Thus, it is imperative that techniques be developed for extracting the maximum amount of diagnostic information from small sets of regional seismic data. This requires a change from the conventional methodology applied to teleseismic data in which detection, location and discrimination are accomplished using a small portion of the seismic data recorded at many stations. Seismic data measured at these distances are generally recorded with usable signal-to-noise ratios only up to frequencies on the order of a few Hertz. Consequently, in the past, it has only been necessary to consider low frequency approximations to the seismic source function, propagation path effects and noise conditions at the recording site. However, in-country stations located at regional distances can be expected to provide usable data at frequencies of 10 Hz or higher. Thus, it is important that the high frequency aspects of the problem be studied in more detail, particularly with reference to single station capability.

The objective of the analyses described in this report has been to provide a quantitative assessment of the current state-of-knowledge regarding the detection, location and classification of seismic events using broadband, three-component data recorded at a single station located in the regional distance range. The seismic detection of fully coupled, underground explosions in a variety of different geologic media is considered in Section II where a simple analytic model is defined and applied to the simulation of the frequency dependent detectability of low yield explosions over regional propagation paths similar to those characteristic of the Eastern U.S. The single station event location problem is addressed in Section III by means of simulations of epicentral distance and source azimuth estimations conducted using regional seismic data measured from both U.S. and Russian events. In Section IV, research relevant to the identification of seismic events using discriminants which can be applied to single station regional seismic data is reviewed with particular emphasis on the evaluation of the applicability of the classical teleseismic discriminants to this distance range. This is followed in Section V by a summary, together with a statement of conclusions regarding our current state of knowledge with respect to these issues.

II. DETECTABILITY OF FULLY COUPLED UNDERGROUND EXPLOSIONS AT REGIONAL DISTANCES

2.1 INTRODUCTION

The factors influencing seismic detectability of underground explosions include the seismic source function, the effects of the propagation paths followed by the seismic energy between the source and the receiver and the seismic noise conditions at the recording site. These factors are reasonably well defined for the narrowband signals typically recorded at teleseismic distances, but are currently much less well constrained over the wider frequency band recordable at regional distances, particularly for areas such as Russia for which little or no regional seismic data are available for analysis. In this section the detectability of fully coupled explosions in various source media will be explored using an analytic detection model similar to that employed previously in the analysis of decoupled explosions (Murphy, 1980). In particular, the analysis will focus on the first arriving P waves using a model which has been normalized with respect to observed data from the 5.3 kt Salmon explosion in salt. The initial P wave arrivals have been selected for analysis both because of their importance with respect to event location and discrimination and because later arriving regional phases of potential interest (e.g. L_g) are generally of comparable or larger amplitude and thus the detectability of the initial P wave generally implies the detectability of multiple phases. As in the previous study, Salmon rather than a Nevada Test Site explosion has been selected as a reference event on the basis of the observation that the characteristics of the crustal and upper mantle regional propagation paths throughout much of central Russia appear to be more similar to those typical of the Eastern U.S. than those of the Western U.S. Thus, in terms of any eventual treaty monitoring with in-

country stations, an Eastern U.S. regional propagation model is the preferred initial approximation.

2.2 DEFINITION OF THE MODEL

Despite many years of research, there is still some residual uncertainty regarding the relative seismic coupling efficiency of underground nuclear explosions in various source media. In particular, the theoretical models required to confidently predict the seismic source function given only the yield and depth of burial of the explosion and the physical properties of the source medium are still in the process of being developed and validated. Consequently, an empirically based prediction scheme is required. For purposes of the present analysis we will adapt the approximate analytic model proposed by Mueller and Murphy (Mueller and Murphy, 1971; Murphy, 1977; Murphy, 1981) in which the seismic source function is characterized in terms of a spherical explosive pressure profile (p(t)) acting on the medium at the radius (r_{el}) at which the medium response becomes linear. The far-field P wave displacement spectrum in a homogeneous medium due to such a source is given by:

$$Z(\omega) = \frac{p(\omega)\ r_{el}}{4\mu r} \qquad \frac{i\omega c}{\omega_0^2 + i\omega_0\ \omega - \beta\omega^2} \qquad (1)$$

where c is the compressional wave velocity in the medium, $\omega_0 = c/r_{el}$, $\beta = (\lambda + 2\mu)/4\mu$, where λ, μ are elastic constants of the medium and $p(\omega)$ is the Fourier transform of p(t). The dependence of the various source parameters on yield (W) and source depth of burial (h) for explosions in "hardrock" source media are taken to be of the form (Mueller and Murphy, 1971; Murphy, 1977):

$$p(t) = \left[P_o\, e^{-\alpha t} + P_{oc}\right] H(t)$$

$$P_{os} \equiv P_o + P_{oc} \sim \rho g h$$

$$r_{el} \sim \frac{W^{1/3}}{h^{1/n}}$$

$$P_{oc} \sim \frac{4}{3}\,\mu \left(\frac{r_c}{r_{el}}\right)^3 \qquad (2)$$

$$r_c \sim \frac{W^{0.29}}{h^{0.11}}$$

$$\alpha \sim \omega_o$$

where $\rho g h$ is the overburden pressure, n is the rate of decay of the peak shock pressure (P_{os}) in the nonlinear regime and r_c is the final cavity radius. It can be seen from equations (2) that one of the limitations of the selected approach is that it requires an initial measurement from a detonation in a particular medium to form a base from which extrapolations can be made to other detonations in that same medium. However, the existing experience data base from U.S. explosions is quite extensive and the proposed model has already been calibrated for explosions in salt, granite, wet tuff/rhyolite (T/R) and shale emplacement media. The calibration data for detonations in these media are summarized in Table 1 and the corresponding far-field displacement spectra (corrected for source crustal structure effects, Murphy, 1978) are compared in Figure 1 for a yield of 1 kt and a standard containment depth of burial of 122 m. Also shown on this figure is an estimate of the corresponding source spectrum for a 1 kt explosion in a dry alluvium/tuff (A/T) medium which is observed

Table 1. Calibration Event Parameters

Source Medium	Calibration Event	n	c, m/sec	ρ, gm/cm^3	W = 1 kt, h = 122 m			
					r_{el}, m	P_{os}, bars	P_{oc}, bars	α, sec^{-1}
Salt	Salmon	1.87	4670	2.20	478	55	8	31
Granite	Shoal	2.40	5500	2.55	321	46	24	34
Tuff/Rhyolite	Various NTS	2.40	3500	2.00	202	36	50	26
Shale	Gasbuggy	2.40	4320	2.35	265	42	25	42

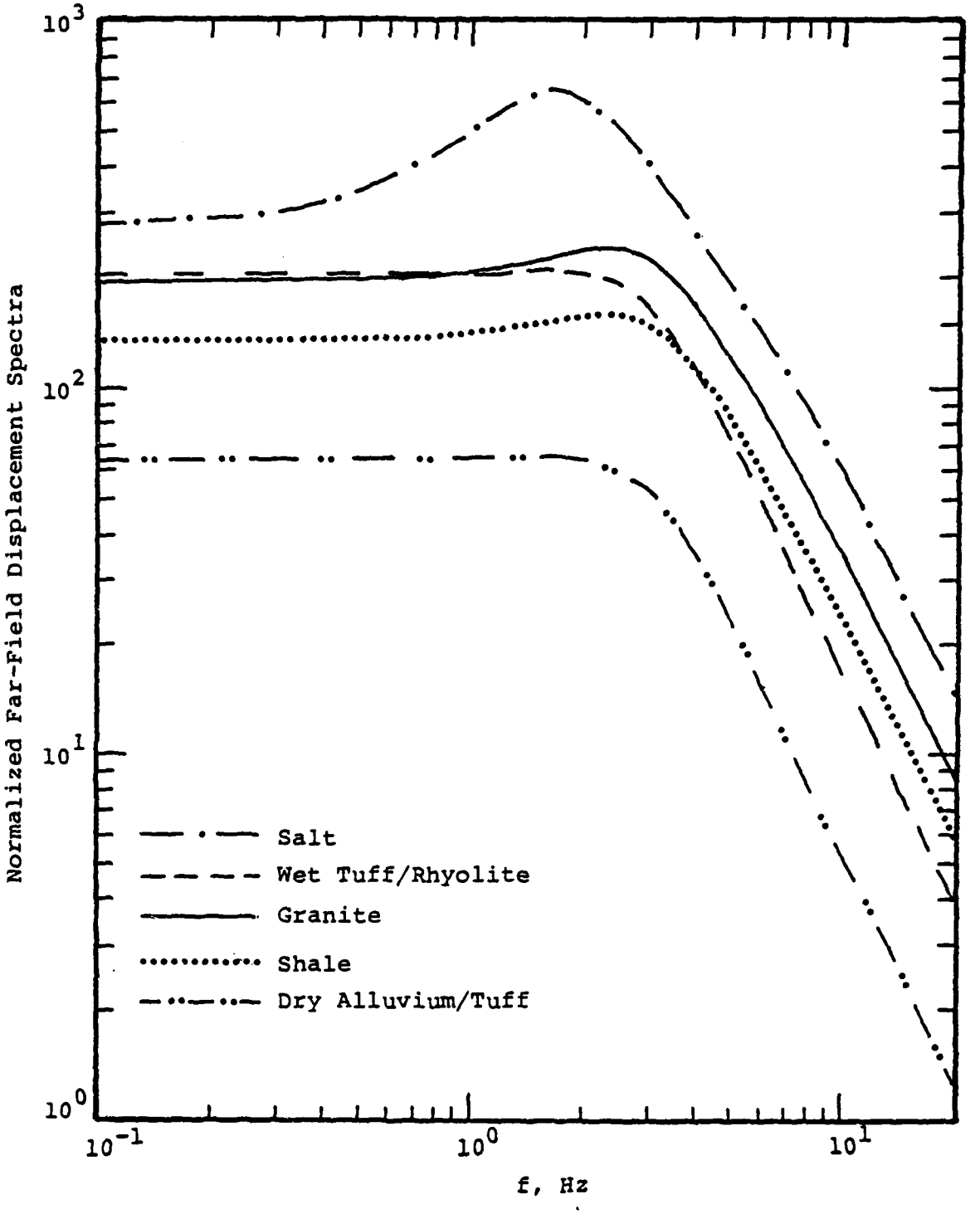

Figure 1. Far-field displacement spectra as a function of source medium, corrected for near-source crustal structure, W = 1 kt, h = 122 m.

to provide the lowest coupling in U.S. experience. Although the Mueller/Murphy source model has not been explicitly calibrated against explosions in such media, it is well documented that the m_b/yield data for explosions in dry A/T consistently fall below those of explosions of the same yield in wet T/R by 0.50 ± 0.25 magnitude units. Although this factor is only indicative of coupling differences in the vicinity of 1 Hz, where m_b is determined, we have approximated the dry A/T far-field displacement spectrum by simply scaling down the corresponding wet T/R displacement spectrum by 0.5 magnitude units (i.e. by a factor of about 3.2), independent of frequency. It will be shown subsequently that the detection of low yield explosions in dry A/T is governed primarily by frequency components in the 2-3 Hz range and thus that the proposed seismic source function, calibrated at 1 Hz, should provide a reasonable approximation for detection analyses. It can be seen from Figure 1 that the spectra for explosions in wet T/R, granite and shale are predicted to be quite similar, while explosions in salt are predicted to couple significantly better and explosions in dry A/T significantly less well than those in the other three media. Note that the predicted difference in coupling between salt and dry A/T is as much as a factor of ten within the frequency range of interest with respect to regional detection. While the five media represented in Figure 1 do not exhaust all source environments of potential interest, experience suggests that the range of coupling represented by these media probably encompasses all those likely to be encountered in test ban monitoring. Consequently, they have been adapted to define the range of seismic source functions to be used in the parametric detection studies described in this report.

The seismic source functions shown in Figure 1 give a picture of the relative seismic coupling efficiency between explosions in various media. However, in order to assess

detection thresholds it is necessary to incorporate models of the seismic propagation path and recording site noise conditions. As was noted above, the propagation model will be based on the P_n phase propagation in the Eastern U.S. and calibrated against the observed Salmon data. The observed Eastern U.S. Salmon P wave amplitudes (vertical component) are displayed as a function of epicentral distance in Figure 2 (Jordan et al., 1966). It can be seen that although the data are widely scattered, the average trend is generally consistent with the r^{-2} decay exemplified by the dashed lines, labeled "optimistic" and "pessimistic" (with respect to detectability), corresponding to the approximate upper bound mean levels which have been selected for analysis purposes. The "optimistic" level is meant to be representative of the model a conservative evader would have to adopt to guard against detection at even a few isolated stations. A selection of the "pessimistic" level, on the other hand, would imply an acceptance of an approximately 50% probability of detection.

Thus, the observed Salmon P wave data can be used to establish the amplitude level and low frequency geometrical attenuation rate for P waves in the Eastern U.S. However, in order to extend the propagation model to higher frequencies, it is necessary to incorporate the frequency dependent attenuation associated with the fact that the transmission medium is not perfectly elastic. This will be accomplished using a standard linear attenuation operator of the form

$$e^{-\frac{\omega r}{2cQ}}$$

where r is the path length, c the propagation velocity and Q is the specific attenuation constant. Thus, our final model for the P wave signal, $S(\omega)$, has the form:

$$S(\omega) = A_0 \frac{Z(\omega)}{r^2} e^{-\frac{\omega r}{2cQ}} \qquad (3)$$

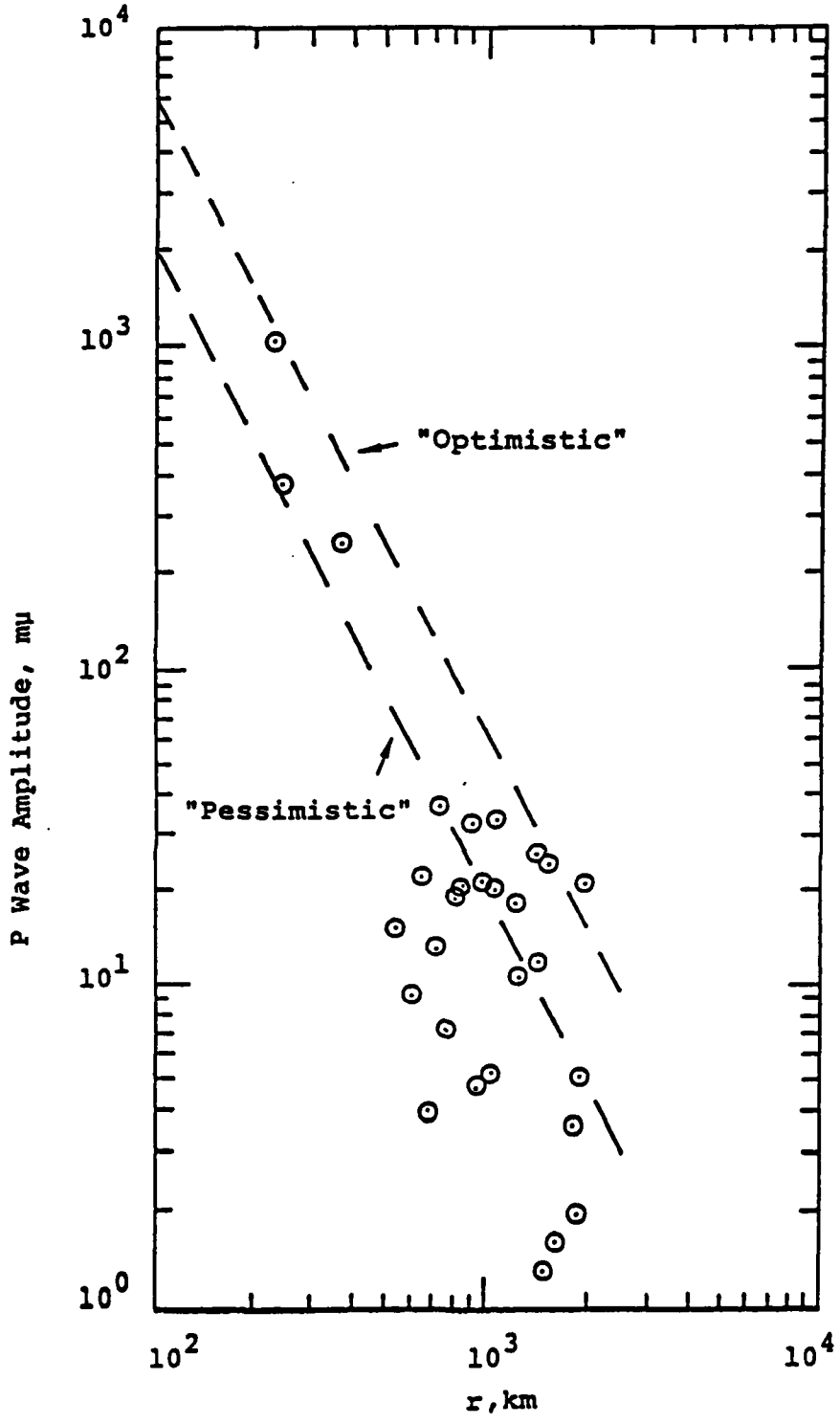

Figure 2. Salmon P wave amplitudes as a function of epicentral distance.

where A_0 is an amplitude constant chosen to be consistent with the observed Salmon P wave data (i.e. the "optimistic" and "pessimistic" levels of Figure 2), $Z(\omega)$ is one of the far-field P wave displacement spectra from Figure 1, c = 8.5 km/sec and Q is either 1500 ("optimistic") or 750 ("pessimistic") (Murphy, 1980).

Given the signal level as a function of frequency and range (i.e. equation (3)), it remains to specify the expected background noise level at the receiver so that signal-to-noise (S/N) ratios can be computed and used as a basis for assessing detectability. As in the previous study (Murphy, 1980), the "optimistic" (again with respect to detectability) noise spectrum is chosen to correspond to a 2 mμ peak-to-peak noise level at 1 Hz and an f^{-2} frequency dependence. The selected "pessimistic" noise spectrum is simply the optimistic estimate multiplied by a factor of five and thus corresponds to a 10 mμ peak-to-peak displacement at 1 Hz.

Since the adopted model is tied to Salmon experience, it follows that its predictions should be consistent with the P wave observations from this 5.3 kt explosion in salt. Figure 3 shows the predicted Salmon S/N ratios as a function of frequency and range computed by combining the "optimistic" (left) and "pessimistic" (right) model elements. It can be seen that the "optimistic" model predicts that Salmon would be detectable over the entire regional distance range, at least for frequencies in the 0.8-5.0 Hz range. This agrees with the observation that Salmon P waves were detected well out into the teleseismic distance range (i.e. $\Delta > 50°$). The "pessimistic" model, on the other hand, predicts that Salmon would not be detectable beyond about 1600 km, which is clearly a conservative estimate with respect to the observations from this event. Thus, the adopted model appears to provide estimates of detectability which are reasonable for efficient regional propagation paths such as those typical of stable

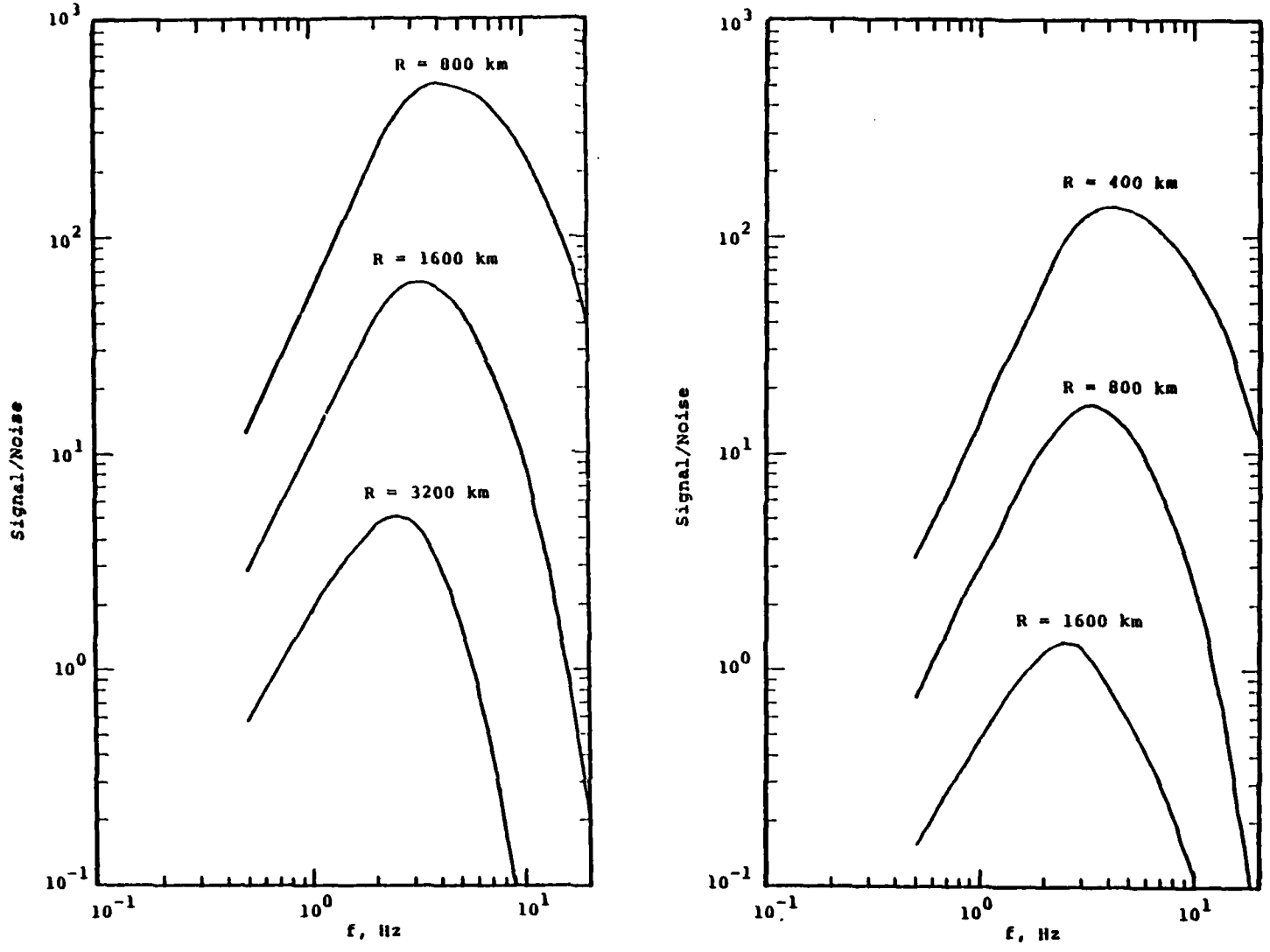

Figure 3. Salmon signal-to-noise ratios as a function of frequency and range predicted using the "optimistic" (left) and "pessimistic" (right) detection models.

tectonic environments typified by the Eastern U.S.

2.3 DETECTABILITY OF UNDERGROUND NUCLEAR EXPLOSIONS AT REGIONAL DISTANCES

The detection model described in the previous section will now be applied to the analysis of hypothetical low-yield explosions in the various source environments represented in Figure 1. In the following discussion, detectability will be associated with a S/N ratio of 1.0 under the assumption that sophisticated signal analysis and possible array processing might be expected to improve the S/N ratio to some extent. In any case, it will be demonstrated that the exact specification of this threshold level plays a relatively minor role in the assessment of detectability. The predicted S/N ratios as a function of range at 0.5, 1.0, 2.0, 4.0 and 8.0 Hz for a 1 kt explosion at a depth of 122 m in salt are shown in Figure 4 for the "optimistic" and "pessimistic" parameter combinations. It can be seen that the "optimistic" model predicts that frequency components of the signal in the 1.0 to 4.0 Hz range should be detectable throughout the regional distance range while the "pessimistic" model predicts a maximum detection range of about 1500 km at 2.0 Hz. A similar presentation for a 10 kt explosion in salt (at a depth of 122 $W^{\frac{1}{3}}$ m) is shown in Figure 5. It can be seen that for this yield detections would be expected out beyond 2000 km even under the pessimistic assumptions. Thus, it seems clear that under normal background noise conditions, regional detection of explosions in salt with yields above 10 kt should pose no problem and, consequently, the subsequent analyses will focus on the lower yield ranges.

The predicted detectability of 1 kt explosions in the five source media of Figure 1 are compared in Figure 6 for the "optimistic" (left) and "pessimistic" (right) scenarios. In this presentation, the distance (R_{max}) at which the S/N ratio

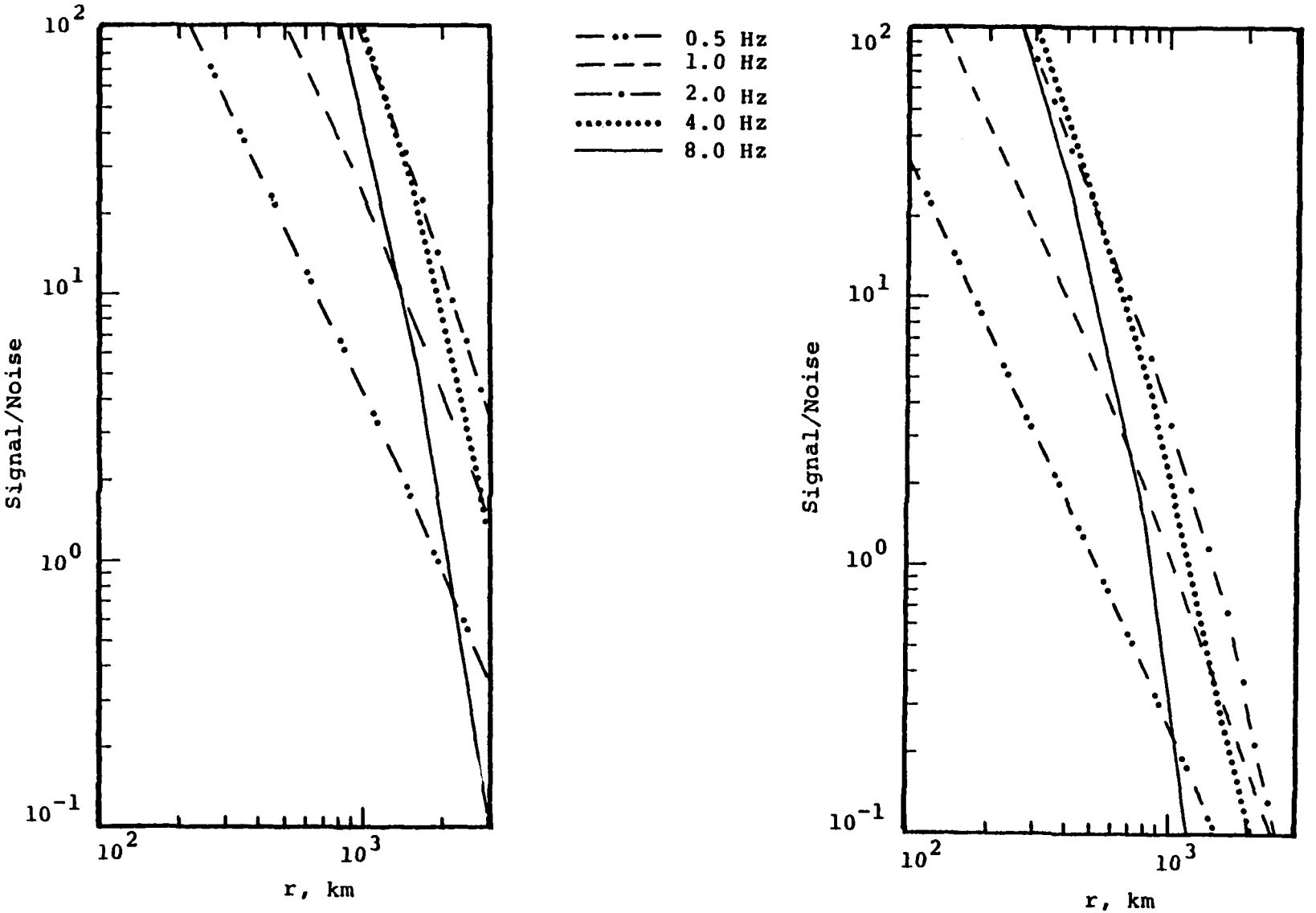

Figure 4. Estimated signal-to-noise ratios as a function of distance and frequency for a 1 kt explosion in salt computed using the "optimistic" (left) and "pessimistic" (right) detection models.

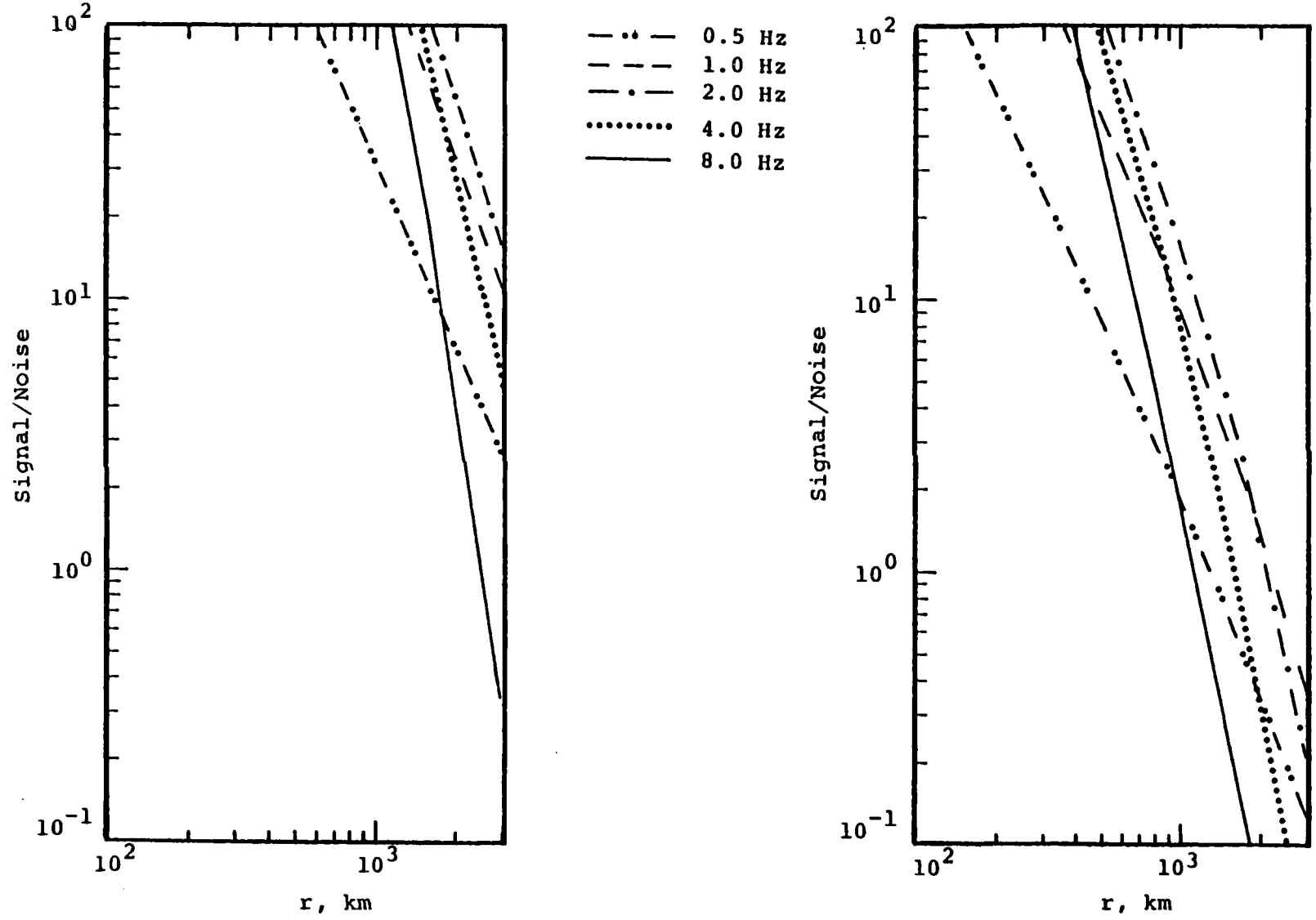

Figure 5. Estimated signal-to-noise ratios as a function of distance and frequency for a 10 kt explosion in salt computed using the "optimistic" (left) and "pessimistic" (right) detection models.

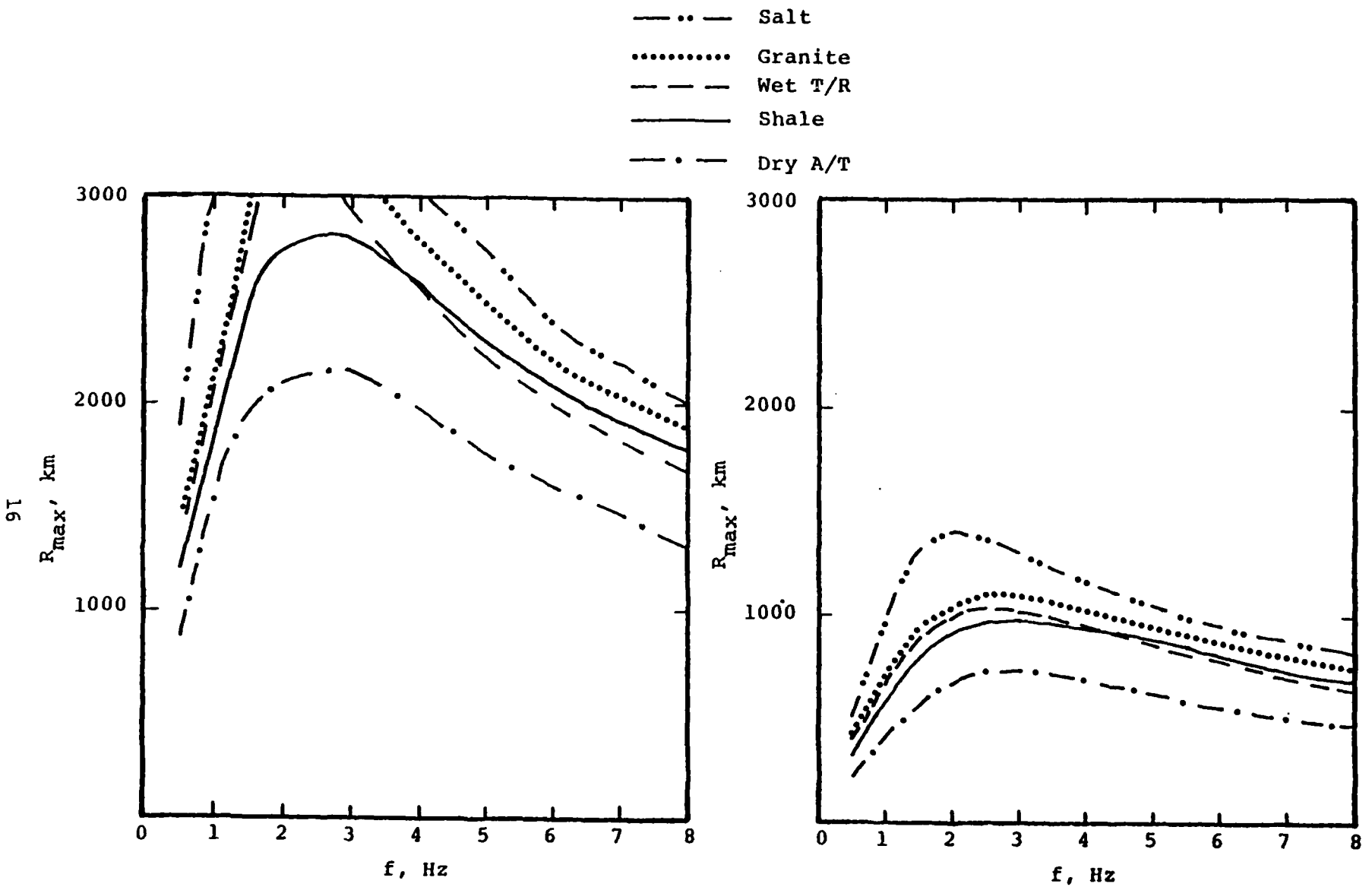

Figure 6. Maximum ranges for detection of 1 kt explosions in various source media as a function of frequency estimated using the "optimistic" (left) and "pessimistic" (right) detection models.

drops to 1.0 is plotted as a function of frequency. It can be seen that, in contrast to the decoupled explosion scenarios considered previously (Murphy, 1980), the frequency components which define the limits of detectability for 1 kt coupled explosions lie in the 2-3 Hz range. This reflects the fact that at this yield the corner frequencies of the source functions all fall below 3.0 Hz (cf. Figure 1) with the signal level decreasing as f^{-2} above this frequency. Thus, for the adopted detection model, the S/N will decrease above this frequency whenever inelastic attenuation is operative (i.e. $Q < \infty$). Note also from Figure 6 that detectability is predicted to drop off sharply below about 2.0 Hz due to the predicted increase in noise level at low frequency. While this is not necessarily important with regard to event detection and location, it has implications with respect to short-period discrimination which will be discussed in a subsequent section. It can be seen from Figure 6 that in terms of the "optimistic" model, even a 1 kt explosion in a dry A/T source medium is predicted to be detectable out to ranges exceeding 2000 km, at least over a limited frequency band. For the "pessimistic" model, the 1 kt explosion in dry A/T is predicted to be detectable only out to about 750 km, but even in this case 1 kt explosions in the other four media are still predicted to be detectable at ranges greater than 1000 km. Note further that although the coupling, and thus the predicted signal amplitude, varies by as much as a factor of ten between explosions of the same yield in salt and dry A/T (cf. Figure 1), the predicted maximum range of detectability varies by only about a factor of two. This effect was noted previously in the analysis of decoupled explosions (Murphy, 1980) and reflects the fact that the signal amplitude decreases as r^{-n} where n is greater than 2.0 due to the combined effects of geometric and inelastic attenuation. Consequently, if the signal strength is increased by a factor F, the range to a fixed S/N

ratio increases only as $F^{1/n}$. It follows then that detectability is controlled primarily by the effective distance attenuation rate of the phase under consideration.

The predicted detection thresholds for 10 kt explosions in the five source environments of Figure 1 are compared in Figure 7. It can be seen that at this yield level, the "optimistic" model predicts that explosions in any of these media would be detectable over the entire regional distance range throughout most of the frequency band of potential interest. In fact, even under the "pessimistic" assumptions, the model predicts that a 10 kt explosion in dry A/T will be detectable at ranges greater than 1000 km.

In summary, the results of the present analysis suggest that P waves from contained explosions with yields as small as 1 kt should be detectable at ranges on the order of 1000 km or more over regional propagation paths similar to those characteristic of the Eastern U.S. Thus, it is reasonable to assume that, under normal background noise conditions, such explosions should be detected by at least one station of any adequate in-country surveillance network. Given such a single station detection, the question then arises as to whether it would be possible to locate and characterize (i.e. discriminate) the source of the recorded motion. These issues will be addressed in the following sections.

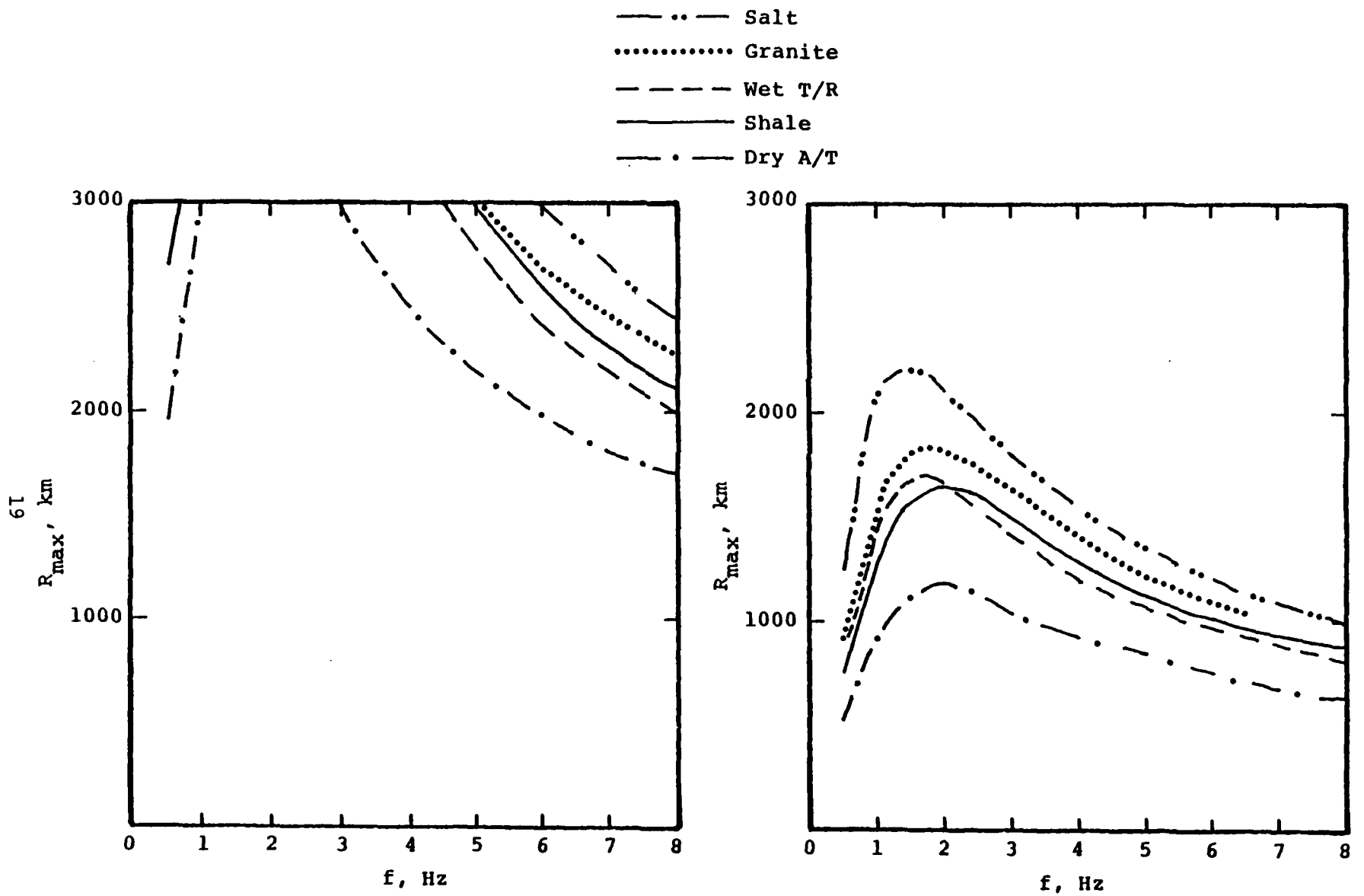

Figure 7. Maximum ranges for detection of 10 kt explosions in various source media as a function of frequency estimated using the "optimistic" (left) and "pessimistic" (right) detection models.

III. EVENT LOCATION USING SINGLE STATION DATA

3.1 STATEMENT OF THE PROBLEM

Seismic event location traditionally involves the use of a large number of first arrival P wave times collected over a range of distance and azimuth. In this approach, a P wave velocity model is proposed on the basis of independent evidence or previous observations and then the hypocentral coordinates are defined as those which, when substituted into the model, provide the best fit to the observed arrival time data. In order to solve for the hypocentral coordinates (i.e. epicenter plus depth) using this algorithm, a minimum of three independent first arrival measurements are required (four if origin time is also to be determined). In fact, routine location procedures often employ dozens of observations which are used to constrain the hypocenter location using a least squares procedure which provides the best overall fit to the observations consistent with the selected velocity model. As with all such procedures, the uncertainty in event location decreases as the number of independent observations increases.

As was illustrated in Section II, the problem with the above procedure in the context of treaty monitoring with in-country stations is that it is unlikely that the required number of initial P wave observations will be available for events down near the detection threshold. This is an important issue, since it is just these events against which we will want to apply other national technical means of verification and this is generally not possible without an estimate of event location. Thus, it is necessary to define procedures for obtaining approximate locations using smaller sets of data. One approach is to use other arrivals in addition to the initial P wave arrival. Thus, for example, since L_g is typically several times larger than P at regional distances, it may be detectable at stations where P is unreadable and a

combination of P and L_g arrival times could then be used for event location purposes. Another approach is to use a variety of arrivals recorded at a single station in conjunction with wave polarization data to derive an approximate location. That is, differences in arrival times of various pairs of phases (e.g. P and L_g, P and S) at a single station are indicative of the distance of the event from the station. The direction of the event relative to the station can then be approximated by analyzing the polarization of various P and surface wave arrivals. For example, for many teleseismic paths, the dominant Rayleigh wave arrivals are expected to produce retrograde elliptical motion in the plane of propagation containing the source and receiver points. Thus, a determination of the particle motion associated with the passage of the Rayleigh wave provides a first order approximation to the source azimuth.

These single-station location techniques have been understood since the earliest days of seismology. However, the relative location accuracy obtainable using these procedures has not been well documented due to the fact that, in order to minimize ambiguities, most research is conducted using data from large events recorded at many stations. In this section some representative sets of single-station regional phase data will be examined in an attempt to illustrate the event location capability associated with such data.

3.2 DETERMINATION OF EPICENTRAL DISTANCE FROM MULTIPLE PHASE ARRIVAL TIME DATA

The procedures for estimating epicentral distance from multiple phase arrival times are well known and quite simple (see, for example, Evernden, 1976). Suppose A_1 and A_2 denote two distinct regional arrivals whose travel times over a given distance range can be approximated by the linear

relations

$$T_{A_1} = \frac{\Delta}{V_{A_1}} + C_1$$

$$T_{A_2} = \frac{\Delta}{V_{A_2}} + C_2 \qquad (4)$$

where Δ denotes the epicentral distance, the V_{A_i} denote the apparent velocities and the C_i are constants incorporating the origin time and possible nonzero intercepts of the travel time curves. It follows from (4) that if the travel time curves are known, the epicentral distance can be approximated from the difference in arrival times of the two known phases:

$$\Delta = \frac{T_{A_2} - T_{A_1}}{\left(\frac{1}{V_{A_2}} - \frac{1}{V_{A_1}}\right)} + C' \qquad (5)$$

For some of the better documented regional phases such as P_n, P_g, S_n, S_g and L_g, regionalized travel time curves are often available which can be used to obtain first approximations to the explicit forms of equation (5). However, in the present context it seems likely that, for a given station of interest, such an initial approximation will ultimately be refined using data actually measured at that station. Therefore, in the simulations conducted in this section, the locations will be made using arrival time relations determined from the arrival time data under investigation. That is, it will be assumed that the station has been calibrated using measured data from regional events. Before proceeding to discuss the simulations, we note, as a point of reference, that in a previous study, Evernden (1976) concluded, that with about 0.90 probability, range to U.S. seismic events can be established to within 6 to 8 km by use of clear P_g and S_g onset times recorded at a single station.

The first example to be considered is the Salmon event which was widely recorded at regional distances in the Eastern U.S. First P wave arrival times for this event have been published by Jordan et al. (1966), and the corresponding arrival times of the maximum L_g phase amplitudes at a few Eastern U.S. stations have been published by Pomeroy (1978a). The derived $t_{L_g} - t_p$ data are shown at the top of Figure 8 where it can be seen that a single straight line adequately fits the observed data over the range from 250 to 2500 km. The best-fit linear relation shown on this figure has been used to estimate the epicentral distance corresponding to each observation and the distribution of the resulting error in epicentral distance, E_Δ, is shown as a histogram at the bottom of Figure 8. This sample is clearly too small to be used to draw any definitive conclusions regarding location accuracy, but it does seem clear that, in this case, the standard error of estimate about the true location is on the order of ± 40 km for stations at an average epicentral distance ($\bar{\Delta}$) of 1400 km. This is quite large with respect to Evernden's quoted 6 to 8 km uncertainty and probably reflects the ambiguity inherent in establishing a characteristic arrival time for a long duration phase such as L_g. In particular, as will be further illustrated in subsequent examples, the use of times of maximum amplitude in place of phase onset times generally leads to rather large uncertainties in the epicentral distance estimates.

Bollinger (1970) read P_g, P_n and S_g/L_g onset times for five central Appalachian earthquakes recorded at a variety of Eastern U.S. seismic stations. The resulting $t_{L_g} - t_{P_g}$ and $t_{L_g} - t_{P_n}$ data are shown at the top of Figure 9. Again, it can be seen that over the range of observation from about 50 to 800 km, the interphase delay times can be adequately represented by the best-fit straight lines shown on the figure. For this data set there appeared to be no consistent differences in the location accuracy obtainable using P_g or P_n, so

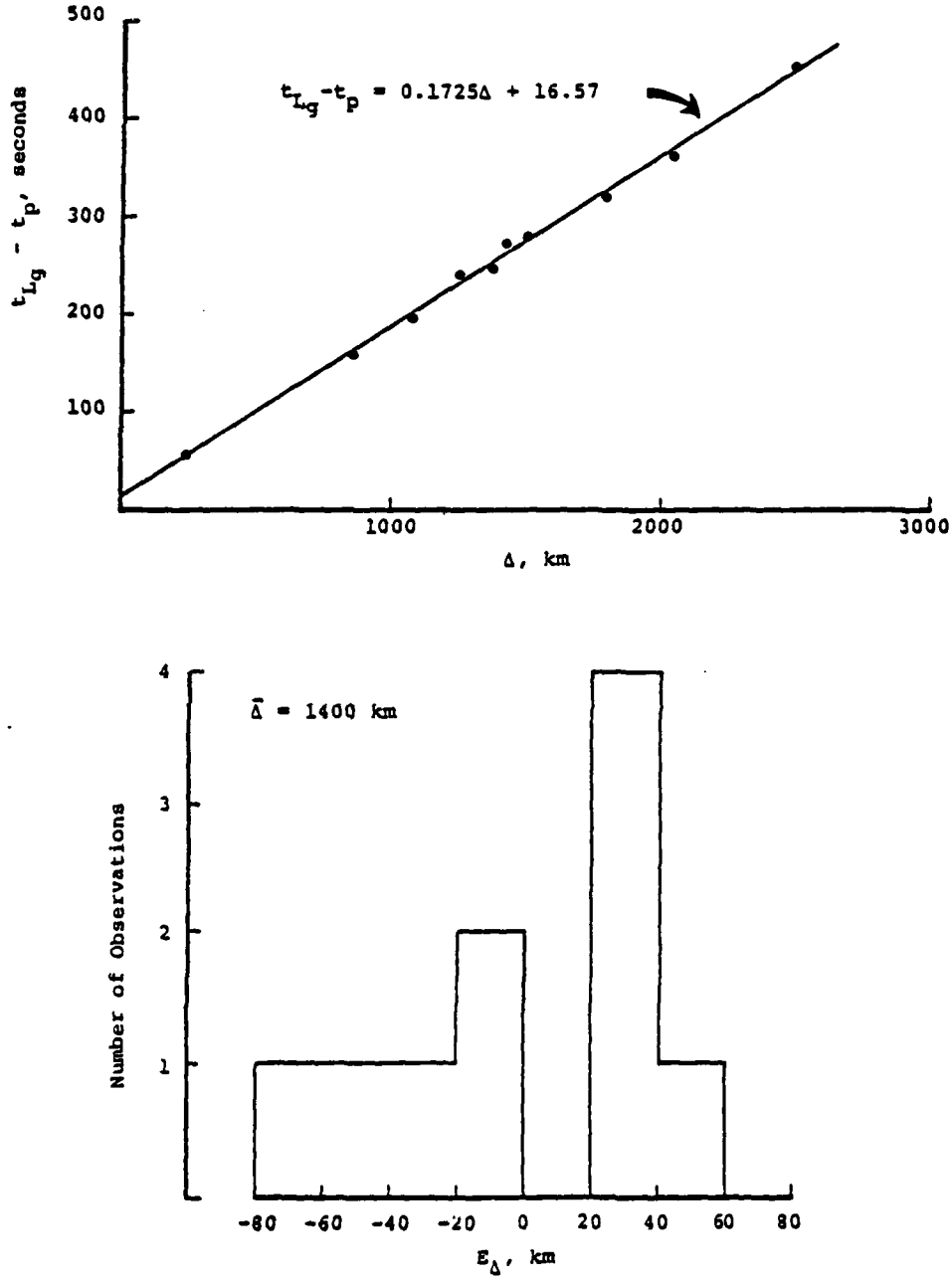

Figure 8. L_g - P arrival time data (top) and single station epicentral distance error distribution (bottom) for Salmon.

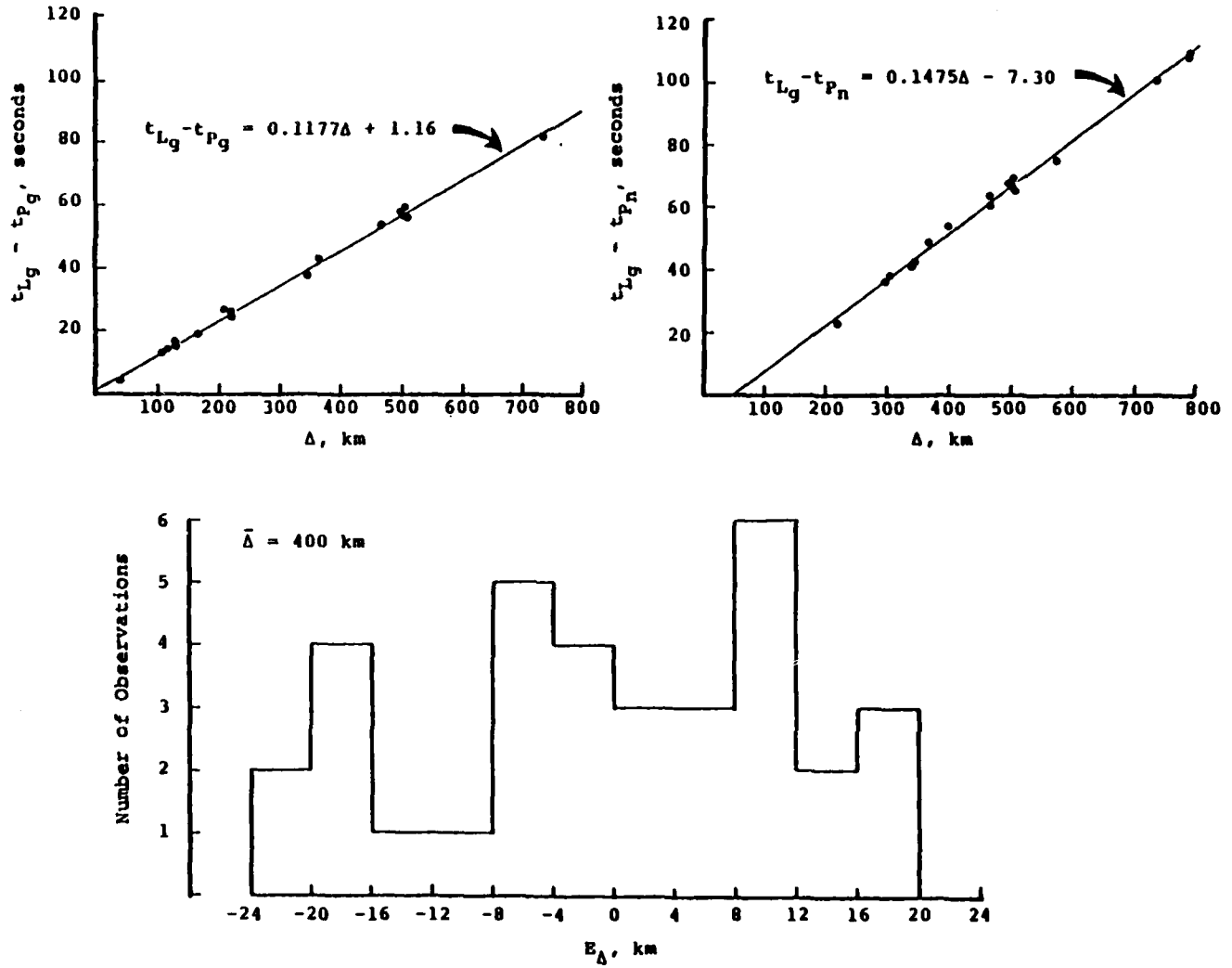

Figure 9. L_g - P_g and L_g - P_n arrival time data (top) and single station epicentral distance error distribution (bottom) for Central Appalachian earthquakes.

the errors in epicentral distance inferred from the two sets of L_g- P data were combined to form the histogram shown at the bottom of the figure. Here the standard error of estimate about the true location is approximately ± 12 km for $\bar{\Delta}$ = 400 km which illustrates the improvement in accuracy that can be obtained if onset times of later phases can be determined.

Figure 10 shows some 140 earthquake S-P times measured at stations in the Central Mississippi Valley seismic network (Stauder et al., 1981). Although this data set is fairly large, it can be seen from this figure that the distance range over which observations are available is limited to about 25 to 350 km, with the bulk of the data concentrated near an epicentral distance of 100 km. Therefore, the location capability quoted here might be considered to be representative of that obtainable at a station located in close proximity to an area of special interest (e.g. salt domes). Note that the data here are best represented by two straight lines with a break occurring at about 160 km. This presumably corresponds to the range where P_n and S_n become the first arrivals. The distribution of the epicentral distance errors derived from these data are shown in Figure 11. Here the standard error of estimate about the true epicentral distance is only on the order of ± 4 km or less for an average epicentral distance of 115 km. Thus, as might be expected, rather precise epicentral distance estimates can be obtained from data recorded at a station in the near-regional distance range.

The next example focuses on multiple phase arrival time data recorded at the Tonto Forest Observatory (TFO) in Arizona from earthquakes located in the vicinity of the Nevada Test Site. For this selected data set, the approach azimuth is essentially constant and the epicentral distance range is limited to about 550 ± 50 km. For purposes of this simulation, the times of occurrence of the maximum amplitudes of the P_n, P_g, S_n and L_g phases have been determined for about 20

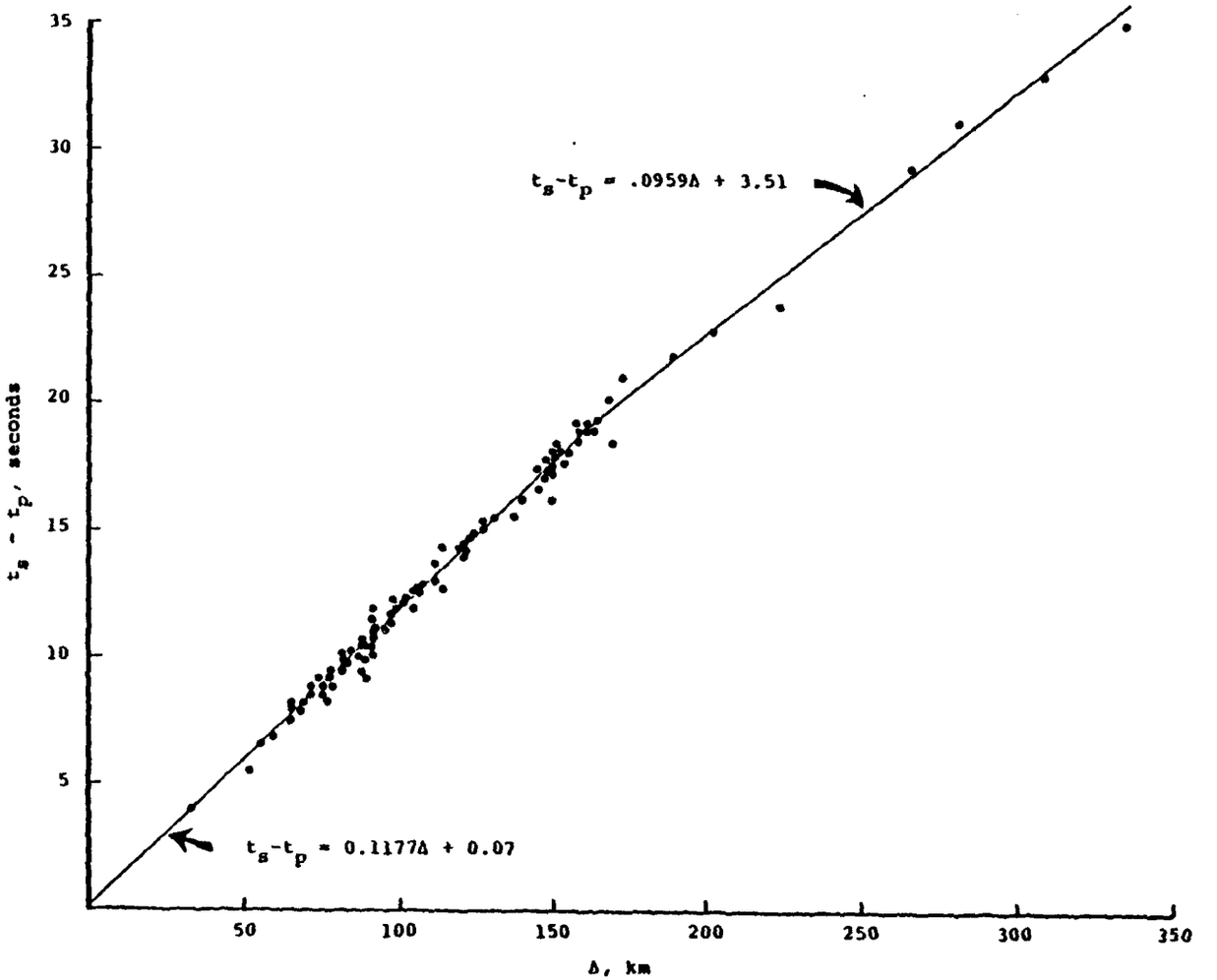

Figure 10. S - P arrival time data from Central Mississippi Valley seismic network earthquake recordings.

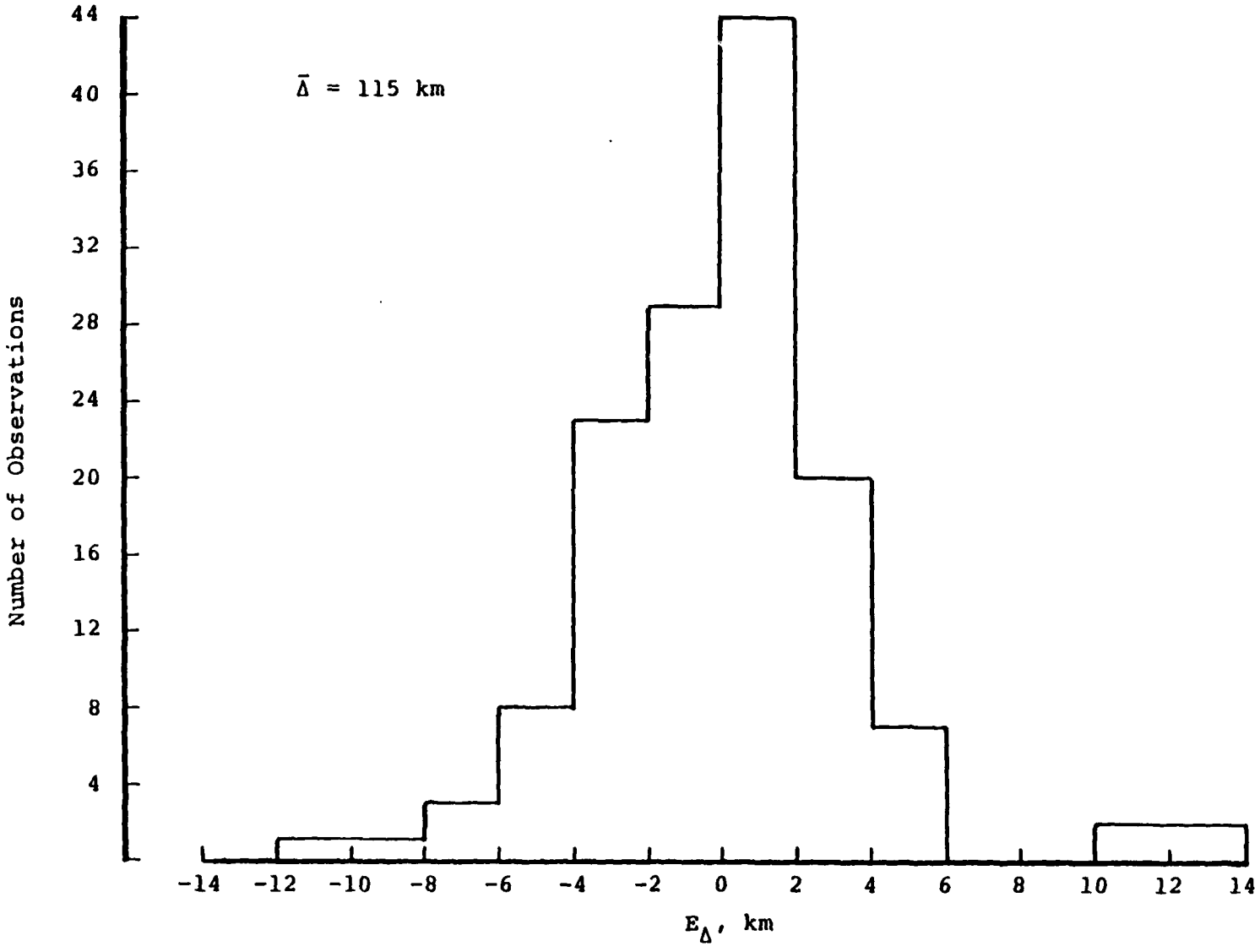

Figure 11. Single station epicentral distance error distribution for Central Mississippi Valley earthquake data.

earthquakes recorded at TFO and the various interphase arrival times have been computed and fit by linear functions of distance as in the previous examples. The corresponding errors in epicentral distance were then computed from the observed data for each combination of phases and the distributions of these errors are shown as histograms on Figures 12 and 13. It can be seen that the error distribution varies considerably depending on which pairs of phases are used for the determination of epicentral distance. On the basis of this small sample, it appears that the best distance resolution for this data set is provided by the $S_n - P_n$ and $L_g - P_n$ interphase arrival time differences, for which the standard errors of estimate about the true epicentral distance are on the order of ± 25 km. The estimates obtained from pairs involving the P_g arrival time are noticeably more scattered, reflecting the fact that the P_g phase is generally not a very distinct arrival at TFO. Again, although the time of occurrence of maximum amplitude is the least ambiguous (and sometimes the only) arrival time reading which can be made, it is clear that the inability to read phase onset times can lead to rather large uncertainties in epicentral distance.

The last example to be considered here is drawn from multiple phase arrival time data recorded at a station in India from earthquakes and presumed explosions in Russia. For these recordings, the same timing procedure employed at TFO was used, with the exception that the S wave onset time, t_{S_s}, was read in addition to the time of maximum S wave amplitude, t_{S_m}, whenever such a reading was possible. The distribution of the computed errors in epicentral distance for the various pairs of observed phases are shown in Figures 14 and 15. Again, as at TFO, there is substantial variability between the epicentral distance accuracy obtained from the various pairs of phases, with pairs involving the P_g arrival giving the greatest scatter. The best estimates are obtained

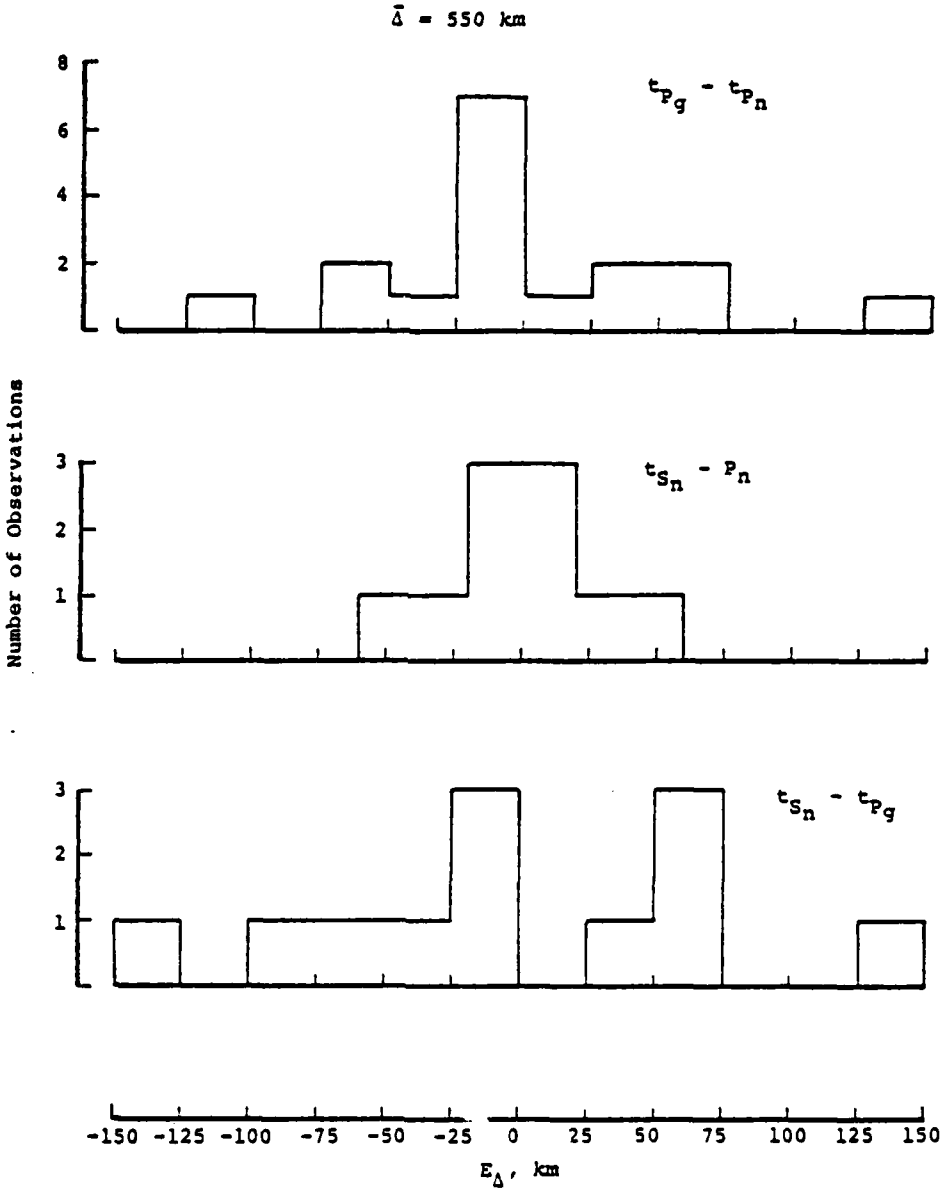

Figure 12. $P_g - P_n$, $S_n - P_n$ and $S_n - P_g$ single station epicentral distance error distributions for Southern Nevada earthquakes recorded at Tonto Forest Observatory.

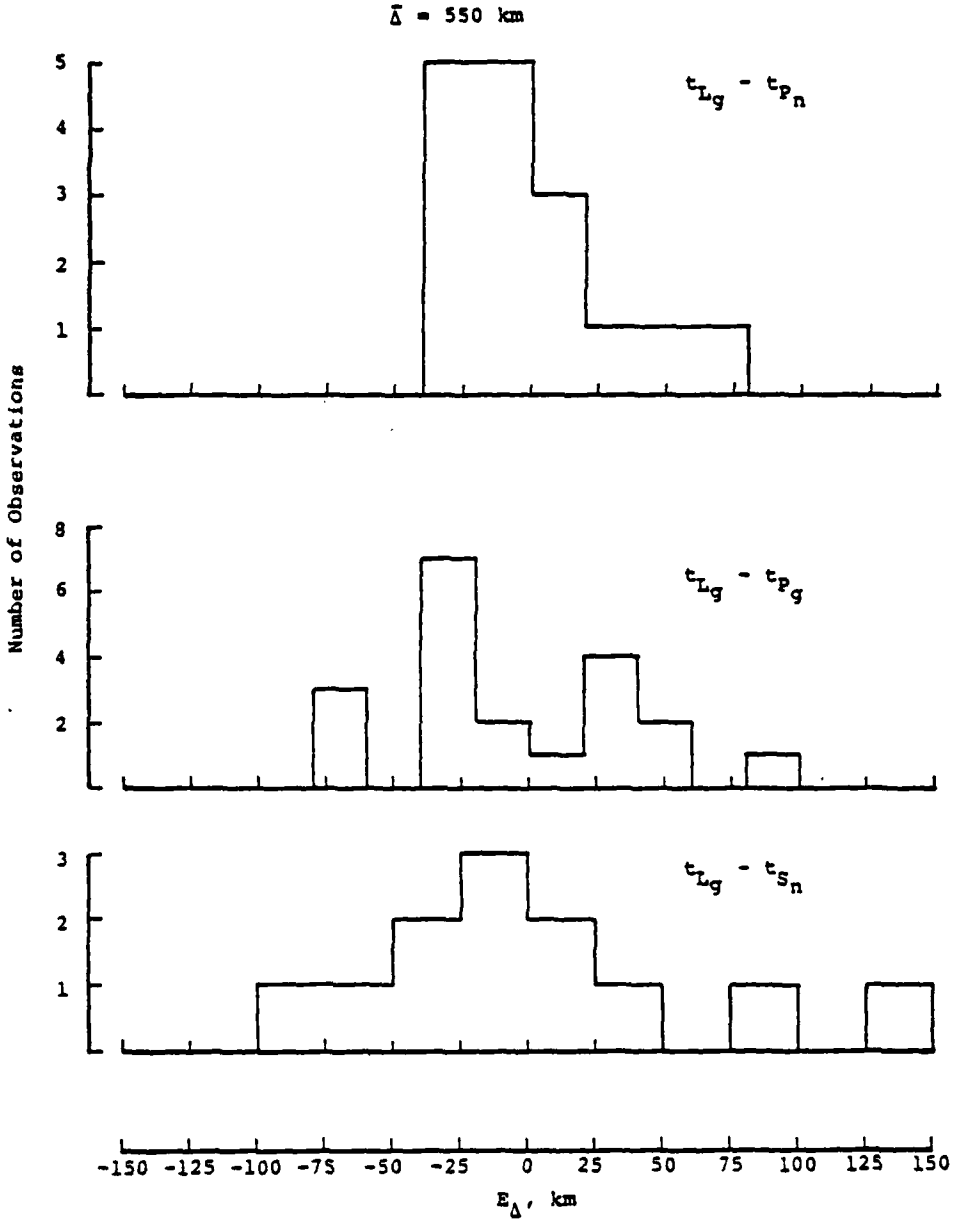

Figure 13. $L_g - P_n$, $L_g - P_g$ and $L_g - S_n$ single station epicentral distance error distributions for Southern Nevada earthquakes recorded at Tonto Forest Observatory.

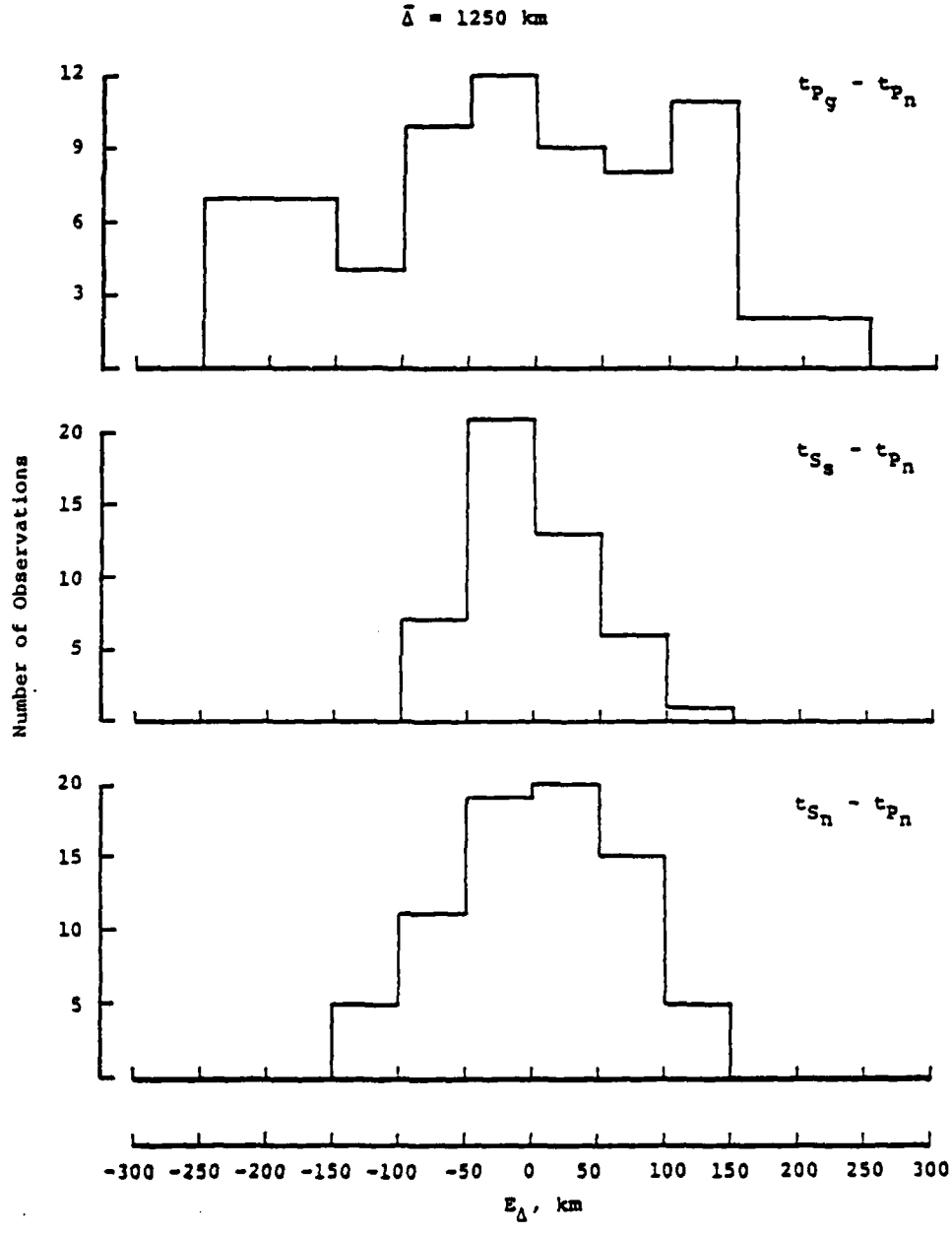

Figure 14. $P_g - P_n$, $S_s - S_n$ and $S_n - P_n$ single station epicentral distance error distributions for Russian earthquakes and explosions recorded in India.

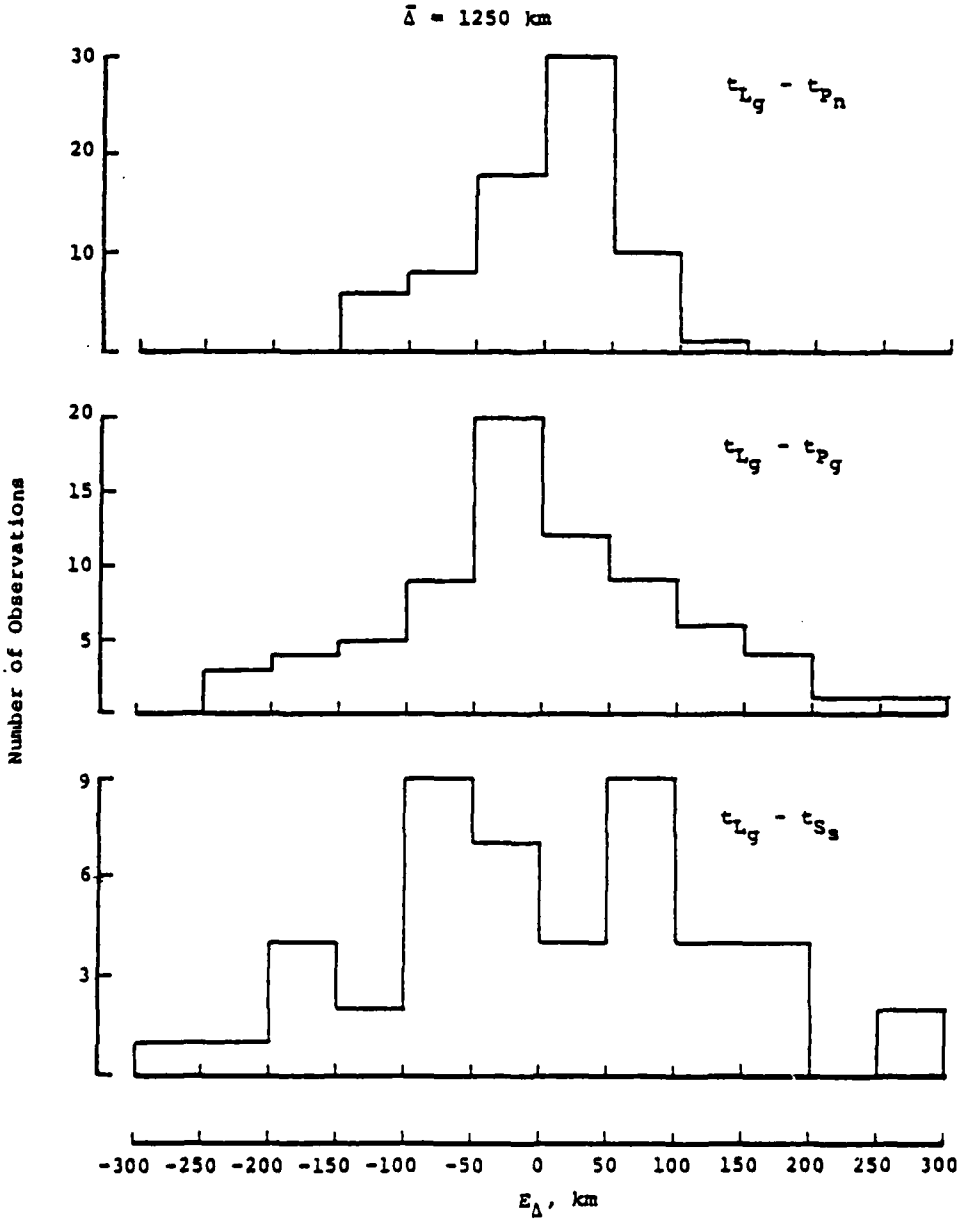

Figure 15. $L_g - P_n$, $L_g - P_g$ and $L_g - S_s$ single station epicentral distance error distributions for Russian earthquakes and explosions recorded in India.

from the $S_s - P_n$ and $L_g - P_n$ pairs, but even here the standard errors of estimate about the true epicentral distance are on the order of ± 50 km for an average epicentral distance of 1250 km. This large uncertainty reflects the fact that for the complicated propagation paths sampled here, the regional phases are not very well recorded and, consequently, it is difficult to make consistent determinations of phase arrival times.

In summary, a variety of interphase regional arrival time data have been examined in an attempt to illustrate the uncertainty in epicentral distance estimates which are encountered when using single station data. Clearly, the data which have been examined to date are not optimum in the sense that they were generally not measured with event location in mind and represent a variety of timing techniques. However, all the times were read by trained seismologists and they serve to indicate some of the problems that might be encountered in an actual surveillance context. In particular, the data suggest that when phase onset times cannot be read due to the indistinct nature of the phase or signal-to-noise problems, it seems clear that the uncertainty in epicentral distance can be substantially greater than the 6 to 8 km quoted by Evernden (1976). In fact, the only data set examined for which accuracies of this order were obtained was for the Central Mississippi Valley Network S-P times observed at an average epicentral distance of only about 100 km. Although the data base examined to date is not sufficient to support definitive, quantitative conclusions, a preliminary estimate might be that epicentral distance can be estimated to within 10 to 15 km (for $\bar{\Delta} \approx 1000$ km) at a calibrated station at which multiple regional phases are well recorded (e.g. over regional propagation paths similar to those encountered in the Eastern U.S.). At stations where the phases of interest are less distinct, and only times of occurrence of maximum

phase amplitude can be reliably determined, the uncertainty in the single-station epicentral distance estimate may be expected to be at least twice this large.

3.3 DETERMINATION OF SOURCE AZIMUTH FROM SINGLE STATION WAVE POLARIZATION DATA

When three-component data are available for analysis, the particle motion can be determined as a function of time as the individual waves pass and, if the waves can be identified, the apparent direction of approach of the waves can be computed, giving an estimate of the source azimuth. For example, P wave particle motion is confined to the plane of propagation and is linear along the ray direction while, as noted earlier, the classical fundamental mode Rayleigh wave particle motion is retrograde elliptical in the plane of propagation. In this section, we will examine some specific examples which illustrate the accuracy obtainable using such azimuth determinations and evaluate some of the sources of uncertainty through detailed analyses of selected Salmon P wave data.

Smart (1978) has recently developed a maximum-likelihood surface wave processor which can be used to estimate source azimuth from three-component recordings of ground motion at a single seismic station. The idea behind this scheme is that an observed surface wave signal can be represented as a superposition of Rayleigh and Love waves. In theory, the Rayleigh wave contributes only to the motion on the vertical (R_Z) and radial (with respect to the source) horizontal (R_H) components, where the horizontal amplitude is related to the vertical amplitude by the Rayleigh wave ellipticity ratio ($\epsilon = R_H/R_Z$) and, for many cases of interest, the horizontal motion leads the vertical by 90° in phase. The Love wave, on the other hand, contributes only to the horizontal motion and only along a direction orthogonal to the vertical plane of propagation. By minimizing the sum of the

squares of the differences between the observed and theoretical components of motion at a selected frequency, the real and imaginary parts of the vertical Rayleigh wave motion are expressed in terms of the Fourier spectrum of the individual motion components at that frequency, the approach azimuth and the ellipticity. These expressions are then substituted back into the original equation for the square of the difference and the result is summed over some selected frequency band. The resulting error expression is then minimized with respect to azimuth to obtain a relation between the approach azimuth, the summation of Fourier spectra of the observed motion components and the ellipticity, which is taken to be known from independent analyses. In fact, the derived relation is a fourth order polynomial which can be solved analytically to obtain an estimate of source azimuth.

One of the initial applications of this signal processor was to the short-period L_g data recorded from the Gnome and Salmon explosions at Long Range Seismic Measurement (LRSM) stations located in the distance range from about 7 to 25 degrees (Smart, 1978). Somewhat surprisingly, the source azimuth estimates obtained from these data were generally quite good, despite the fact that L_g is known to be the result of the superposition of higher mode Rayleigh and Love waves which are not adequately described by the simple fundamental mode theoretical model employed in the derivation of the surface wave processor. The source azimuth estimates determined for Gnome from L_g recordings in the Eastern U.S. are shown in Figure 16. It can be seen that the estimates are quite consistent, with an average azimuth error of only about 7 degrees. Note, however, that in obtaining this estimate of average error, several instances of 180 degree ambiguity, indicated by the reversed arrow heads, have been ignored. These arise as a result of the fact that the superposition of higher mode Rayleigh waves which produce L_g can lead to prograde elliptical motion as

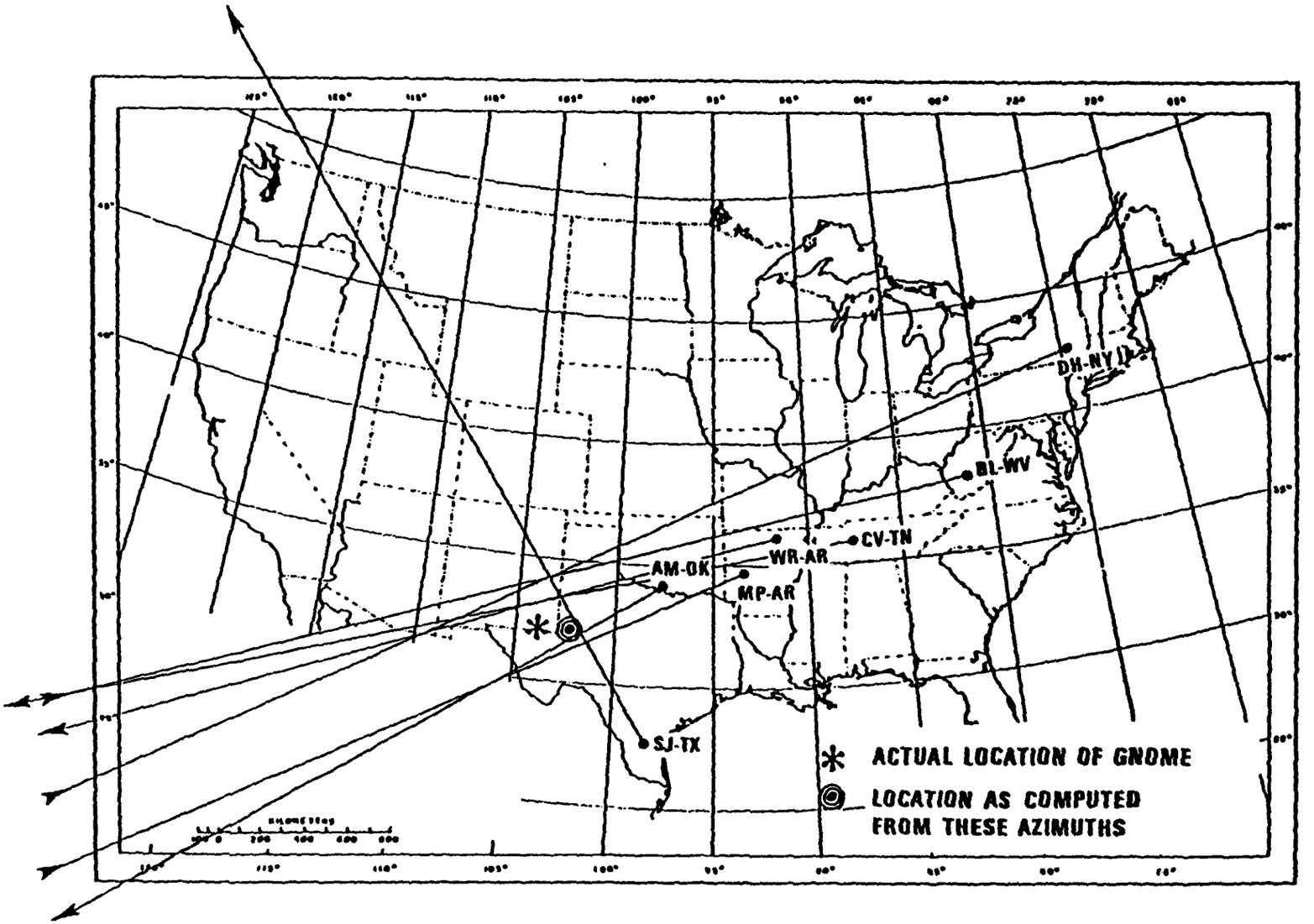

Figure 16. Single station source azimuth estimates determined from Gnome Lg recordings at Eastern U.S. stations (Smart, 1978).

opposed to the classical retrograde motion associated with the isolated fundamental mode Rayleigh waves assumed in the development of the processor. Thus, using single station L_g data alone, the azimuth determination must be considered to contain a 180 degree ambiguity. Smart (1978) also applied the same process to Gnome L_g data recorded at stations in the Western U.S. and the results are shown in Figure 17. Note that the inferred source azimuths shown here display a nearly random pattern and clearly are not useful for event location purposes. This is probably a result of the complexity of the crustal transmission paths in the Western U.S. That is, reflections of energy from lateral discontinuities in crustal structure lead to groups of surface wave energy arriving from a variety of azimuths. These results suggest that the L_g particle motion processor may only be applicable in uniform tectonic regimes such as that typified by the Eastern U.S. Source azimuths determined by Smart (1978) from Salmon L_g recordings at Eastern U.S. stations are shown in Figure 18. Again, with the exception of a notable anomaly at station WFMN in Minnesota, the azimuth estimates are fairly consistent with an average error of about 9 degrees.

Encouraged by the success of these preliminary tests, Smart and Sproules (1981) have recently extended the particle motion analysis to a set of 31 regional events ($\Delta \lesssim 25$ degrees) recorded at station RKON, Red Lake, Ontario (cf. Figure 18 for map location). In this case they found that the average error in the source azimuth determined from L_g was 6.7 degrees (11.1 degrees rms). They also further extended the study by defining a P wave processor which determines the source azimuth and emergence angle by maximizing the mean square vector motion over a selected frequency band. It was found that for this RKON data set, the average error in estimated source azimuth obtained using this P wave processor was only 7.0 degrees (9.1 degrees rms). Thus, in this case, the P wave

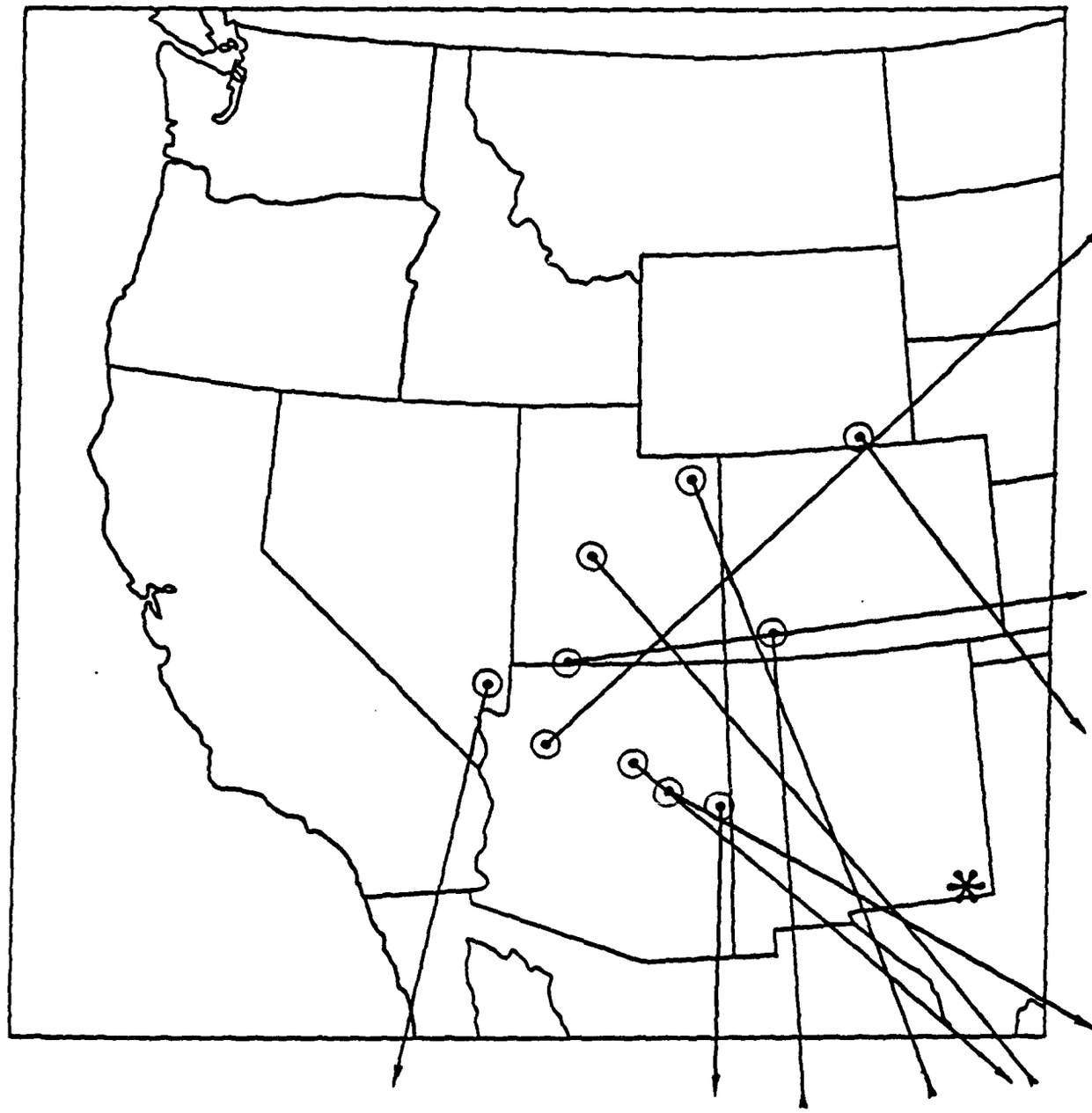

Figure 17. Single station source azimuth estimates determined from Gnome L_g recordings at Western U.S. stations (Smart, 1978).

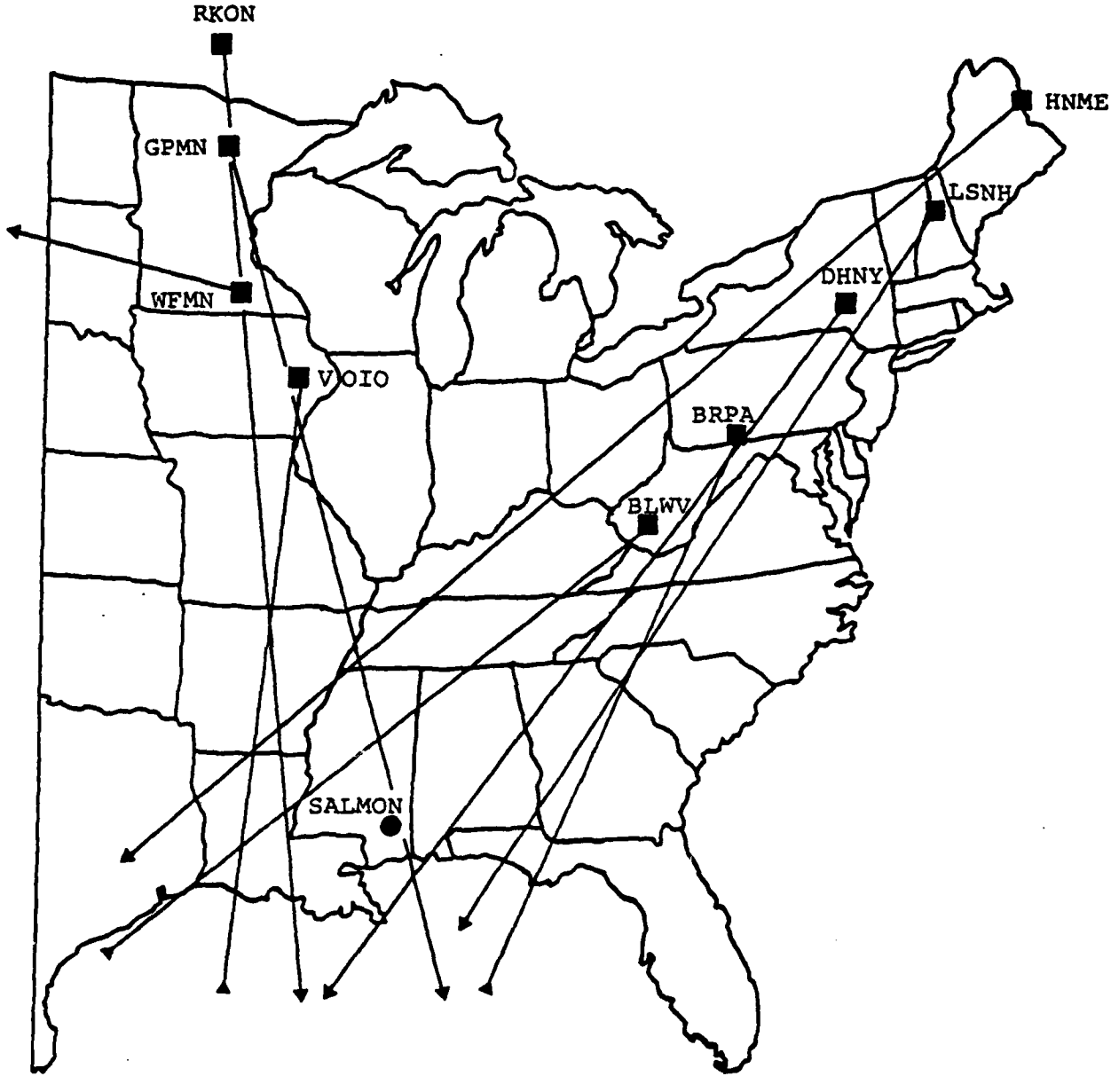

Figure 18. Single station source azimuth estimates determined from Salmon L_g recordings at Eastern U.S. stations (Smart, 1978).

processor gave more accurate results than the L_g processor. Moreover, since it estimates the emergence angle of the wave, P wave particle motion processing with three component data is free of the 180 degree ambiguity in azimuth inherent in the L_g processor. As might be expected, combining the L_g and P wave azimuth estimates increases the accuracy of the process. Thus, Smart and Sproules (1981) found that simple averaging of the two estimates for the RKON data set reduced the average error in the source azimuth to 4.9 degrees (7.0 degrees rms).

We have supplemented the above analyses by applying the P wave processor developed by Smart and Sproules (1981) to initial P wave arrivals recorded from the Salmon explosion at the Eastern U.S. stations used by Smart (1978) in his analysis of the L_g arrivals from this event. In this case, time windows extending 3.2 seconds beyond the first arrival were analyzed and source azimuths were estimated by maximizing the mean square vector motion over the frequency components for which the signal-to-noise ratio was greater than 2.0. The results are shown in Figure 19 where it can be seen that fairly consistent estimates of source azimuth were obtained. Specifically, the average error in source azimuth determined from the P wave particle motion data is 9.5 degrees (11.4 degrees rms), which is nearly identical to that obtained from the corresponding L_g data. Note, however, that the P wave data from all stations could be included whereas for the L_g data the estimate for station WFMN was highly anomalous (cf. Figure 18) and, consequently, was excluded from the average error estimate.

As an example of the data used in the Salmon analysis, the vertical component P wave window selected at station RKON is shown in Figure 20 where a number of subwindows (1-4) have been identified for subsequent reference purposes. The amplitude spectrum computed from this time window is shown in Figure 21 where it is compared with the amplitude spectrum computed from the preceding 3.2 seconds of noise on this

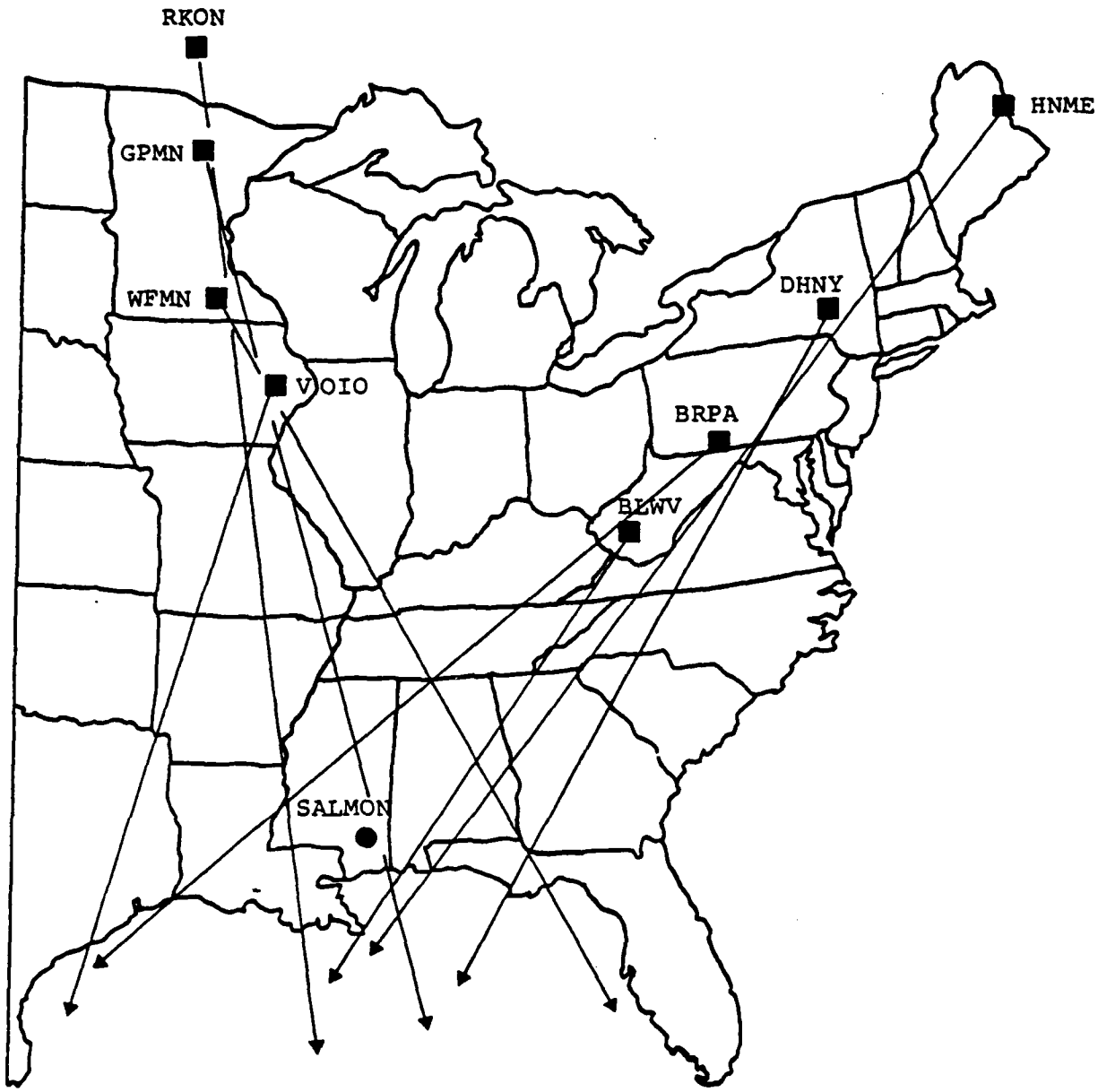

Figure 19. Single station source azimuth estimates determined from Salmon P wave recordings at Eastern U.S. stations.

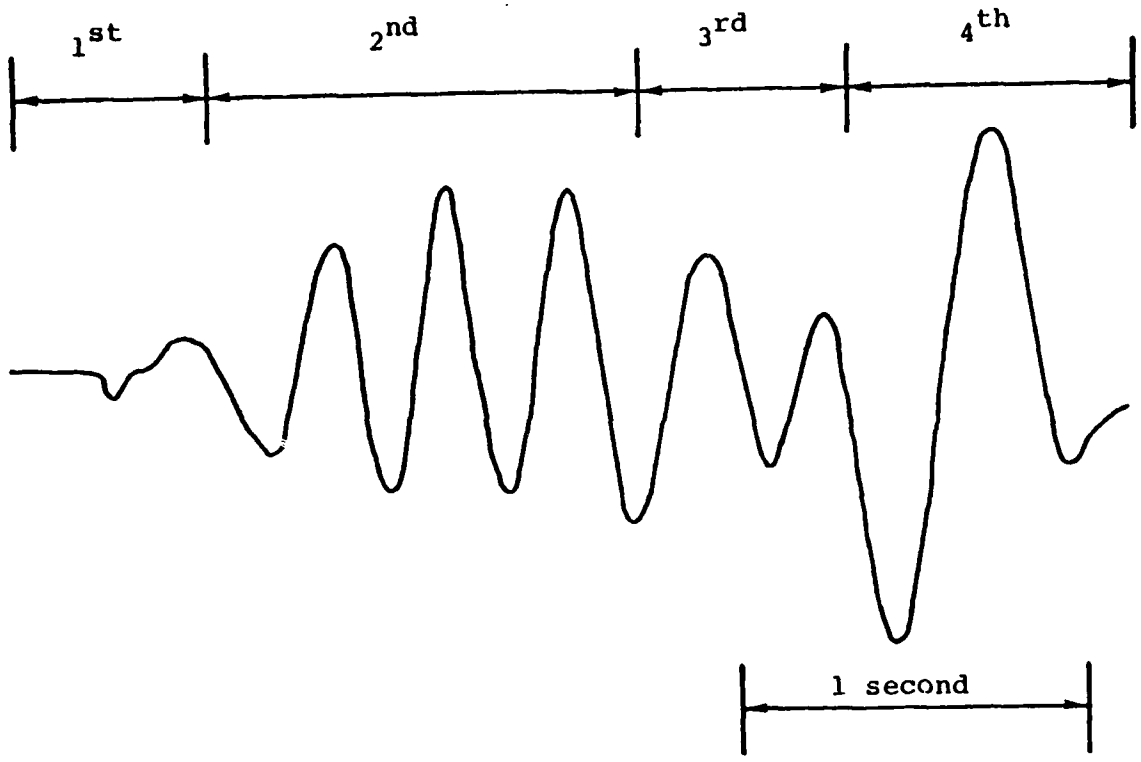

Figure 20. Vertical component P wave recorded from the Salmon explosion at station RKON.

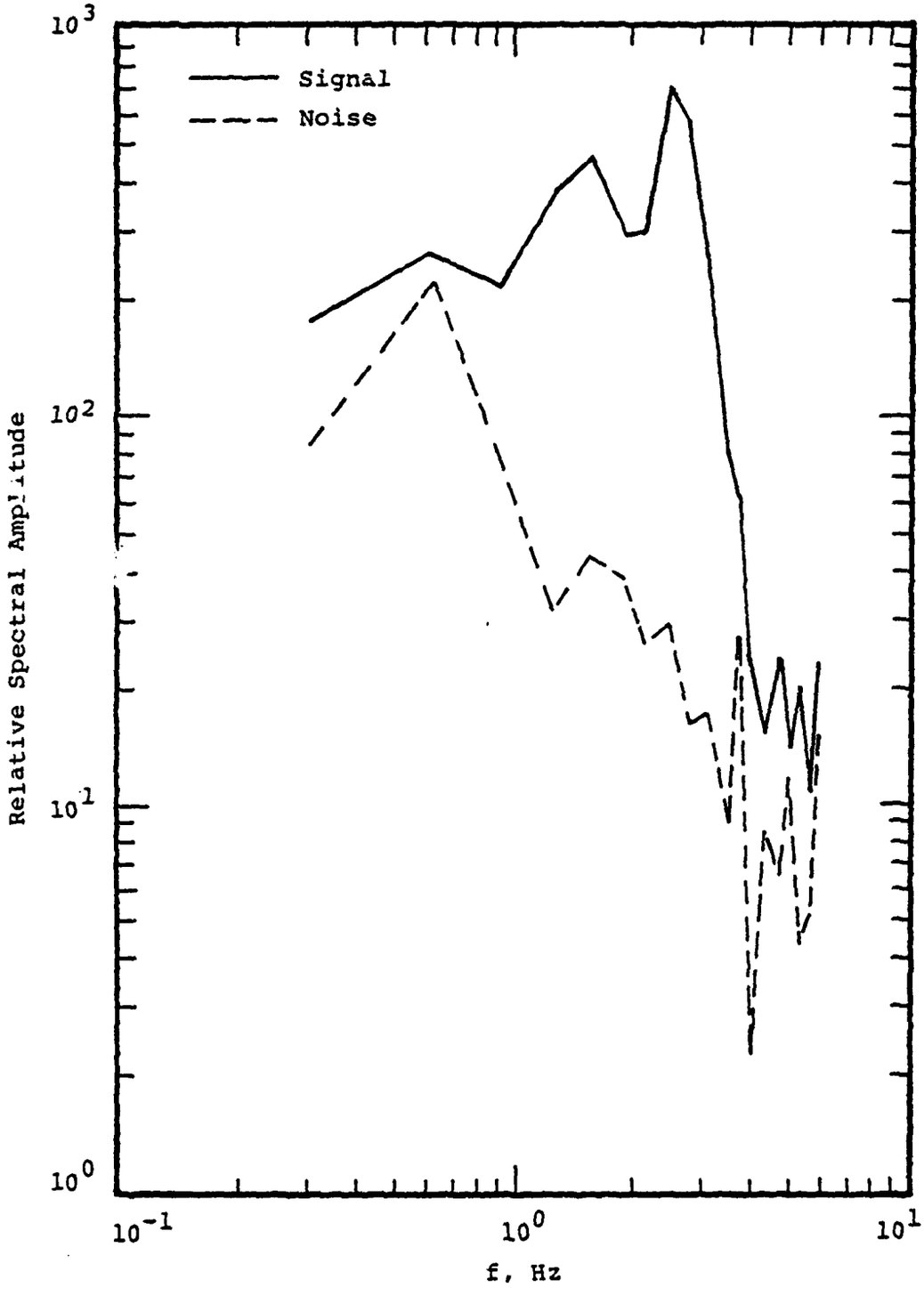

Figure 21. Comparison of Salmon P wave and background noise spectra at station RKON.

record. It can be seen that the signal-to-noise ratio is excellent over the frequency band from about 1 to 4 Hz and this is reflected in the fact that the source azimuth estimated from this portion of the P wave signal recorded at RKON is accurate to within better than 4 degrees. However, it is interesting to note that, even in this case, the particle motion as a function of time is considerably more complicated than that assumed in the simple theoretical model. This is illustrated in Figures 22-25 which show the evolution of the particle motion in the inferred incidence plane (Z vertical, H radial) for the four subwindows identified on Figure 20. Figure 22 shows the particle motion history in the first time window and, since this window is predominantly background noise, it is not surprising that the motion does not resemble that expected from a simple P wave. Figure 23 shows the particle motion history for the second window of Figure 20, which clearly encompasses the initial P wave arrivals. It can be seen that the motion is predominantly linear, as expected. However, it can be seen from Figure 24 that this linearity breaks down in the third time window, indicating that the wave arriving dominating the motion here is not a P wave from the source azimuth. Finally, in the fourth time window, the motion again becomes predominantly linear, indicating the arrival of a secondary P wave from the source azimuth. Thus, even within the first 3.2 seconds of the recording, there is evidence of a complex sequence of arrivals which complicates the determination of source azimuth and probably contributes significantly to the errors in the P wave estimates such as those shown in Figure 19. This suggests that some improvement may result through the use of a phase isolation processor such as MARS (Masso et al., 1979), which has the capability to analyze the spectral composition of individual P wave arrivals.

In summary, available evidence suggests that particle

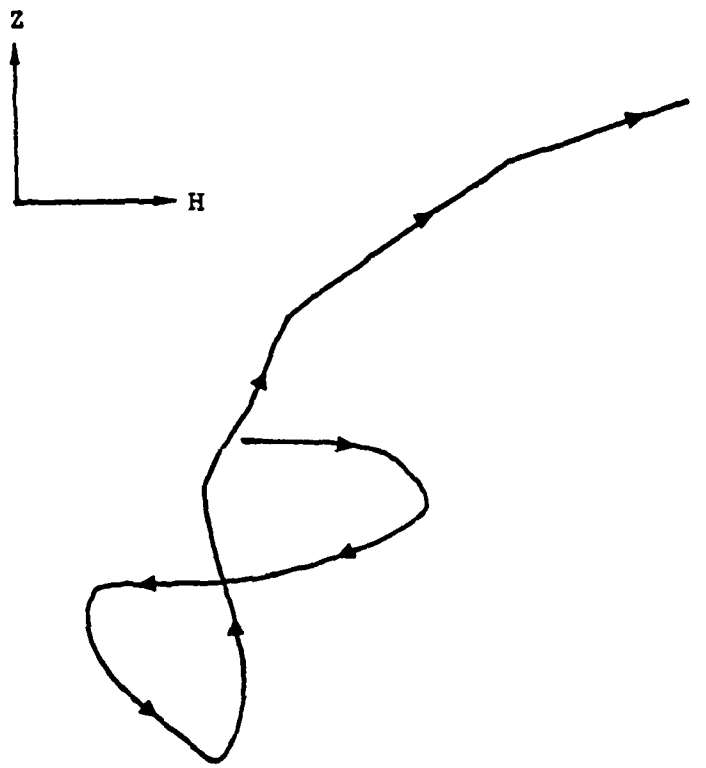

Figure 22. Particle motion diagram in vertical-radial (Z-H) plane for first Salmon P wave window at RKON (cf. Figure 20).

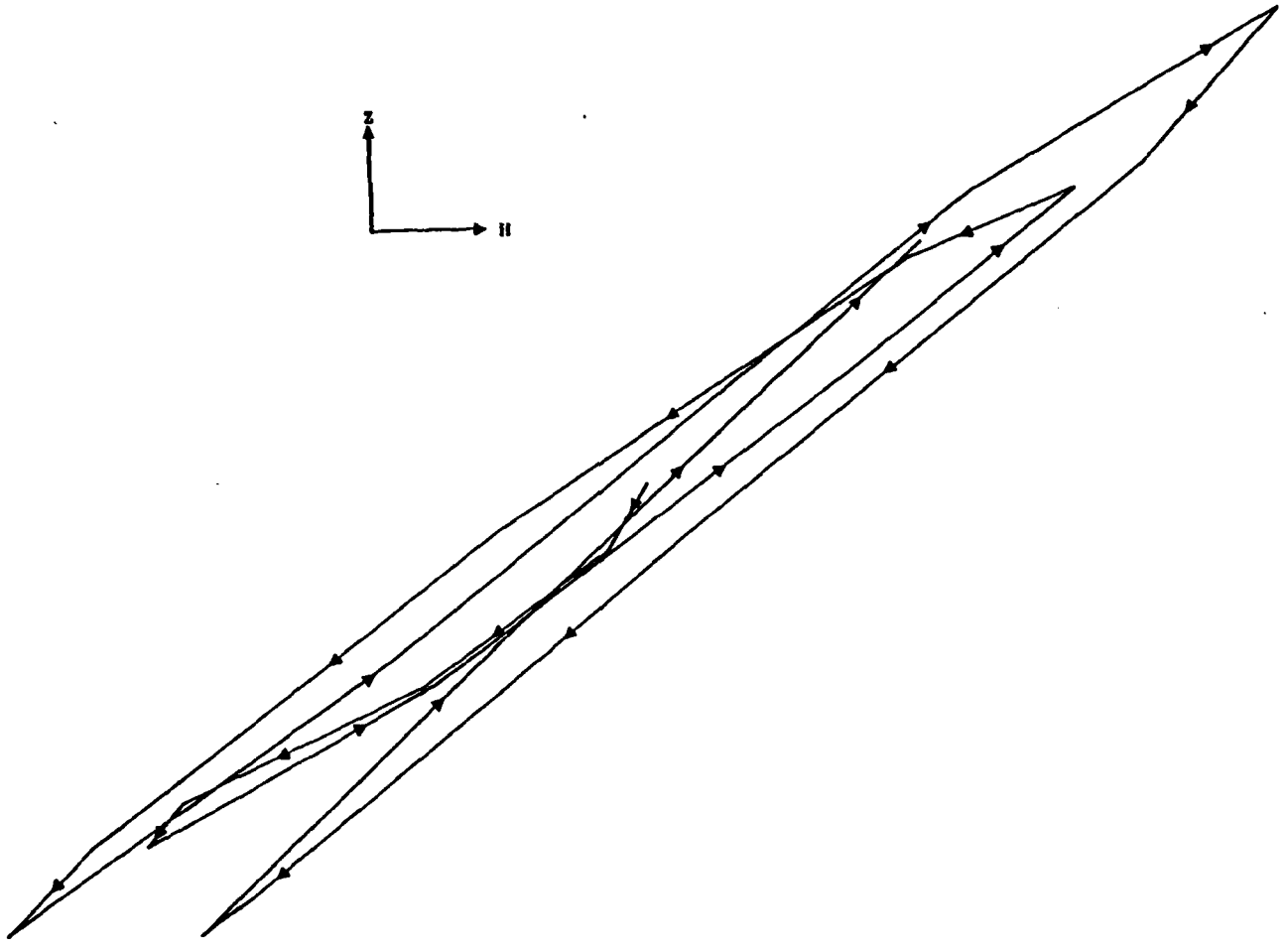

Figure 23. Particle motion diagram in vertical-radial (Z-H) plane for second Salmon P wave window at RKON (cf. Figure 20).

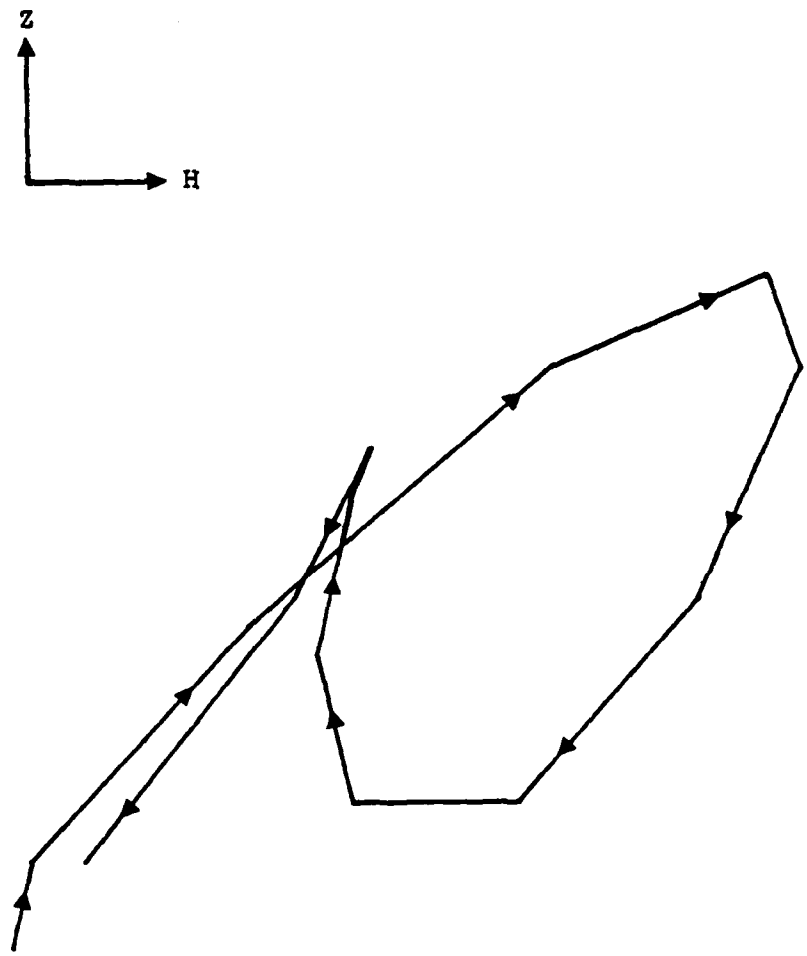

Figure 24. Particle motion diagram in vertical-radial (Z-H) plane for third Salmon P wave window at RKON (cf. Figure 20).

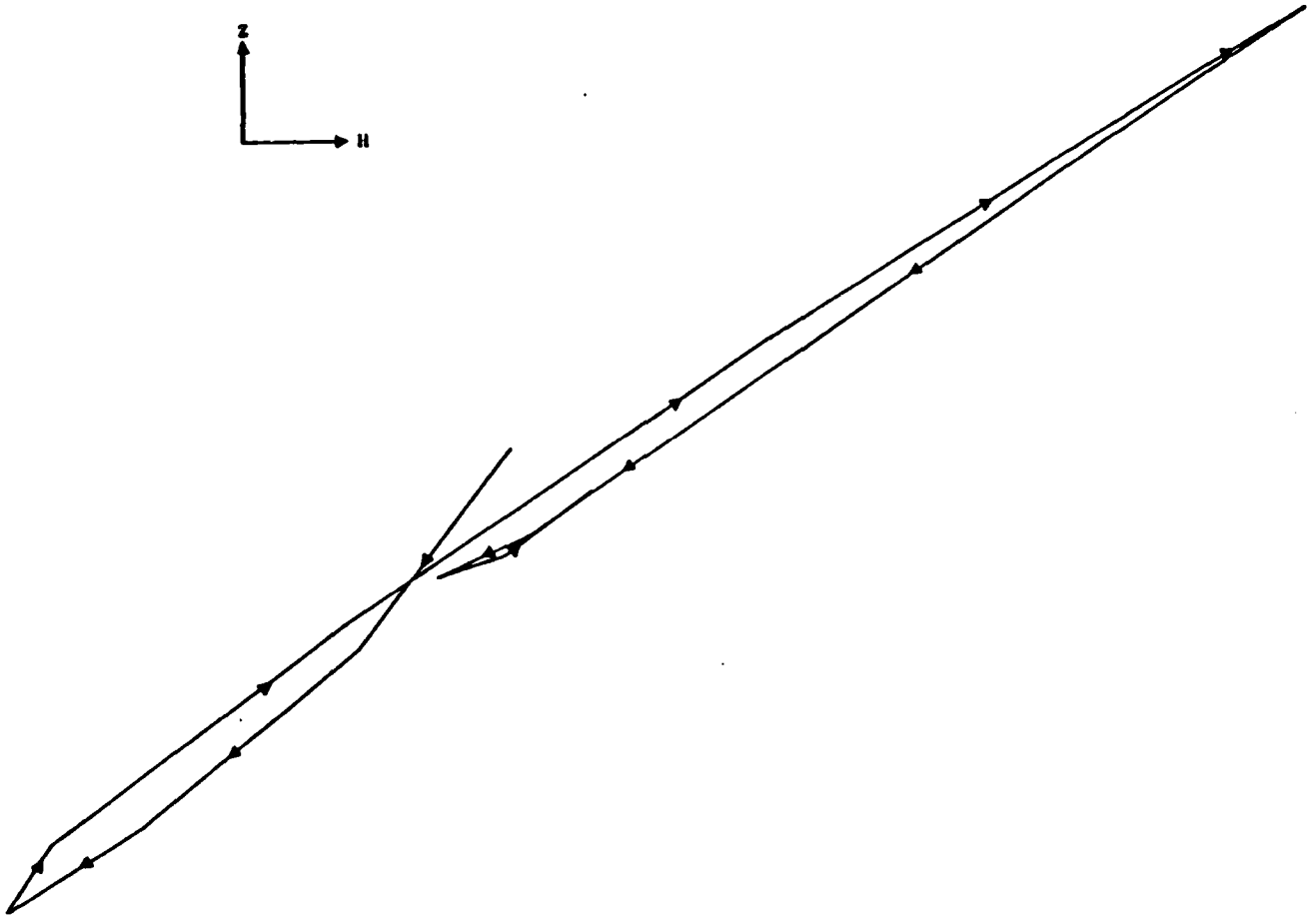

Figure 25. Particle motion diagram in vertical-radial (Z-H) plane for fourth Salmon P wave window at RKON (cf. Figure 20).

motion processing of three component regional phase data recorded at a single calibrated station should permit a determination of source azimuth with an accuracy of better than 10 degrees, at least over fairly homogeneous regional propagation paths such as those typical of the Eastern U.S. This is in essential agreement with an earlier estimate provided by Evernden (1976) on the basis of his analysis of P wave data from U.S. seismic events. At a range of 1000 km an azimuth error of 10 degrees translates into a location error of about 175 km. This is large with respect to the uncertainty in single station estimates of epicentral distance (which may be of the order of ± 15 km) and suggests that additional research in this area should be focused on improving estimates of source azimuth using more sophisticated signal processing techniques.

IV. SINGLE STATION DISCRIMINATION

4.1 INTRODUCTION

As a result of research conducted during the past decade, it now appears that the majority of well-recorded seismic events can generally be identified as being either tectonic or explosive in origin on the basis of analyses of teleseismic data alone. However, due to the existence of detection thresholds and a variety of conceivable evasion techniques, it seems clear that any truly satisfactory monitoring system will have to incorporate seismic data recorded at regional distances. Thus, in the context of the present study, the question arises as to the degree of reliability with which seismic events can be discriminated (i.e. be identified as being either natural or explosive in origin) using data recorded at a single station in the regional distance range. That is, given that an event has been detected and approximately located using single station data, what is the probability that it can be correctly identified using currently available analysis techniques? This is a difficult question in that extensive research has only recently been initiated on the development of a regional discrimination capability and many of the proposed discriminants have not yet been adequately tested. In particular, it is not clear at this time to what extent the various well-tested teleseismic discriminants can be adapted to the analysis of regional data. Basically, there are four well-documented teleseismic discriminants to be considered: focal depth, M_s/m_b, short-period P wave spectral ratios and P wave complexity. In addition to these, some evidence has been presented which suggests that the amplitude ratio L_g/P may be a useful discriminant at regional distances. With regard to single station data recorded at regional distances, it seems likely that the focal depth and P wave complexity discriminants will be of secondary importance. That is, it is well known that single station depth determination

capability is very weak (Evernden, 1976), and it has been observed that both earthquakes and explosions exhibit complex P wave codas at regional distances, presumably as a result of crustal multipathing. Therefore, in the present analysis we will focus on assessing the appliability of the L_g/P, M_s/m_b and short-period P wave spectral discriminants to the classification of regional seismic data.

4.2 L_g/P AMPLITUDE RATIOS

Analysis of the discrimination potential associated with regional P and L_g phases dates back to the early 1960's (e.g. Willis et al., 1963), but it is only in recent years that systematic studies have been conducted using large samples of regional data recorded from explosions and earthquakes in the Western and Eastern U.S. and Russia. Blandford and Hartenberger (1978) examined data from a variety of U.S. events and concluded that the amplitude ratio of the maximum motion before S_n (i.e. P_{max}) to the maximum after S_n (i.e. L_g) is a powerful discriminant between earthquakes and explosions at regional distances. Specifically, they found that this ratio is larger for explosions than for earthquakes by as much as 0.6 magnitude units, at least for events in the Eastern U.S. Gupta and Burnetti (1980) applied the same analysis techniques to regional data recorded at station KBL, Kabul, Afghanistan from a sample of Russian explosions and earthquakes and reached similar conclusions. Figure 26 shows a plot of their KBL data and it can be seen that, although the data are highly scattered, there is an indication that the mean explosion and earthquakes lines are separated by more than 0.5 magnitude units (i.e. by a factor of about 3.5). However, Pomeroy (1978), using a similar data set composed of Russian earthquakes and explosions recorded at a somewhat different set of stations bordering Russia, found no apparent separation of source type using the L_g/P amplitude ratio criterion. Thus, the evidence regarding the

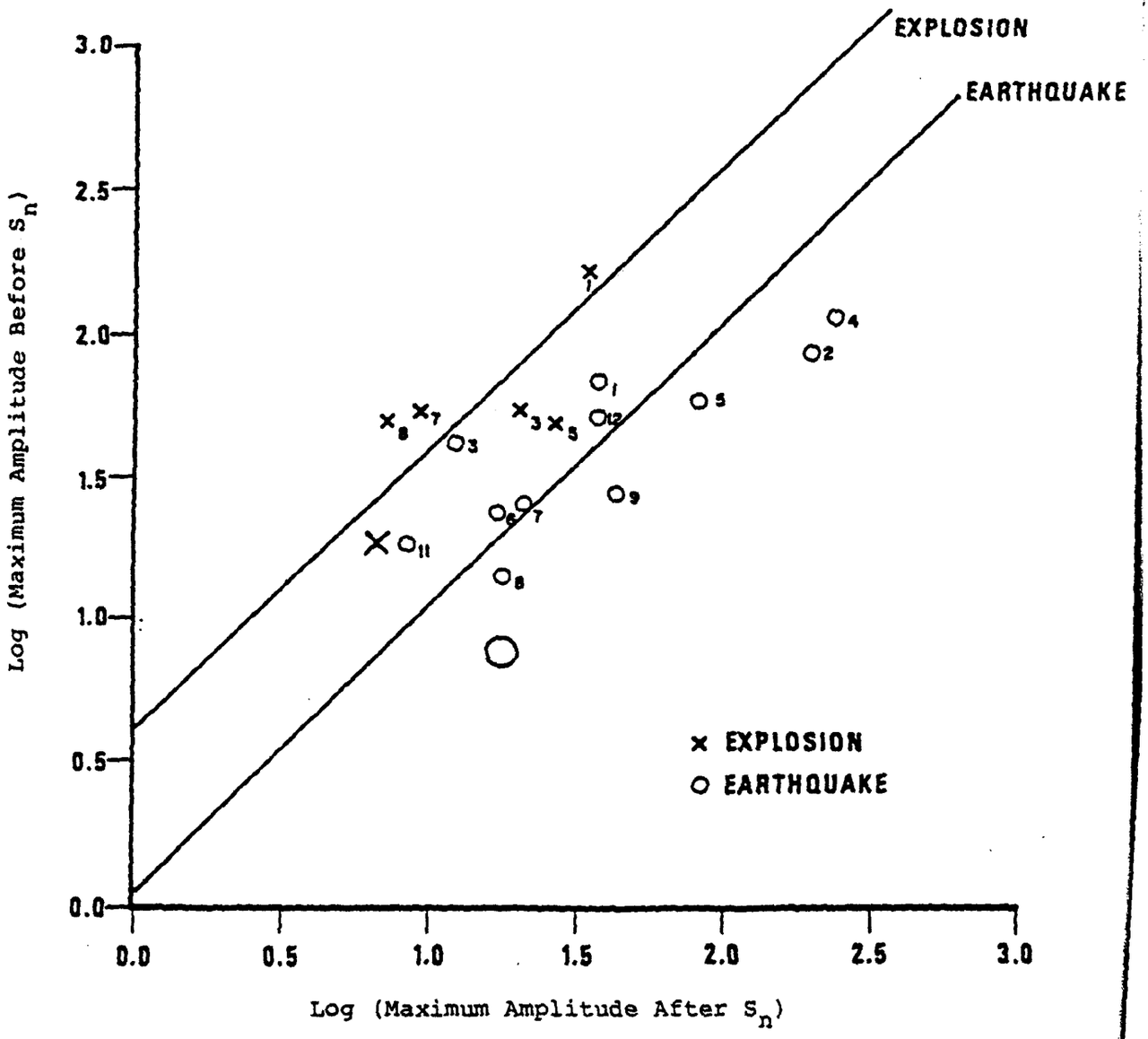

Figure 26. Comparison of P_{max}/Lg amplitude data recorded from Russian explosions and earthquakes at Station KBL, Kabul, Afghanistan (Gupta and Burnetti, 1980).

utility of this regional discriminant is somewhat mixed.

One of the limitations associated with virtually all of the analyses referenced above is that the earthquakes and explosions available for analysis are generally not located in the same areas. Thus, it is not always easy to determine to what extent observed event separations are related to differences in source type versus variable propagation path effects. Bennett and Murphy (1980) have recently attempted to resolve this issue by examining regional data recorded at the Tonto Forest Observatory (TFO) from explosions and earthquakes located in the immediate vicinity of the Nevada Test Site (NTS). Figure 27 shows the locations of the 21 selected earthquakes with respect to NTS and TFO. The data recorded from these earthquakes were analyzed using the same procedures employed by Blandford and Klouda (1980) in their study of regional phases recorded at TFO from NTS explosions. Figure 28 shows the logarithm of the observed P_g amplitudes plotted as a function of the logarithm of the corresponding L_g amplitudes for the 21 earthquakes. Also shown on this figure is the mean line through the earthquake data as well as the mean line through the explosion data determined by Blandford and Klouda (1980). It can be seen that the mean earthquake line lies about a factor of two below the mean explosion line, in qualitative agreement with the findings of Blandford and Hartenberger (1978) and Gupta and Burnetti (1980). However, the scatter in the earthquake data represented on this figure by the 2σ bounds shown as long dashed lines, encompassed the mean explosion line. In fact, the upper 1σ uncertainty bound on the earthquake data nearly coincides with the mean explosion line. This overlap in populations is illustrated more graphically in Figure 29 which shows a comparison of the L_g/P_g amplitude ratios for the 21 earthquakes compared with those from a comparable set of NTS explosions as a function of body wave magnitude m_b. Similar results were found for the L_g/P_n

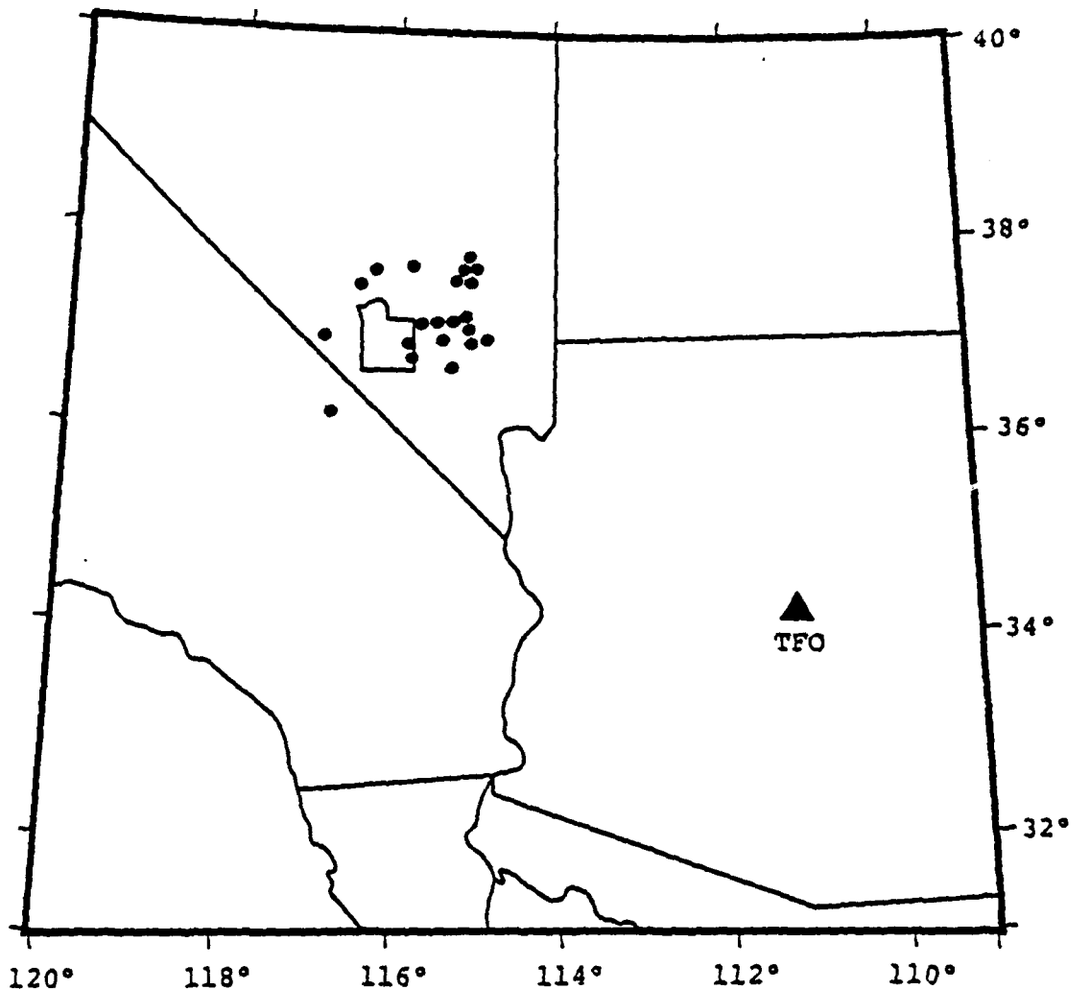

Figure 27. Earthquake source locations (•) used in analysis of regional phase data recorded at Station TFO.

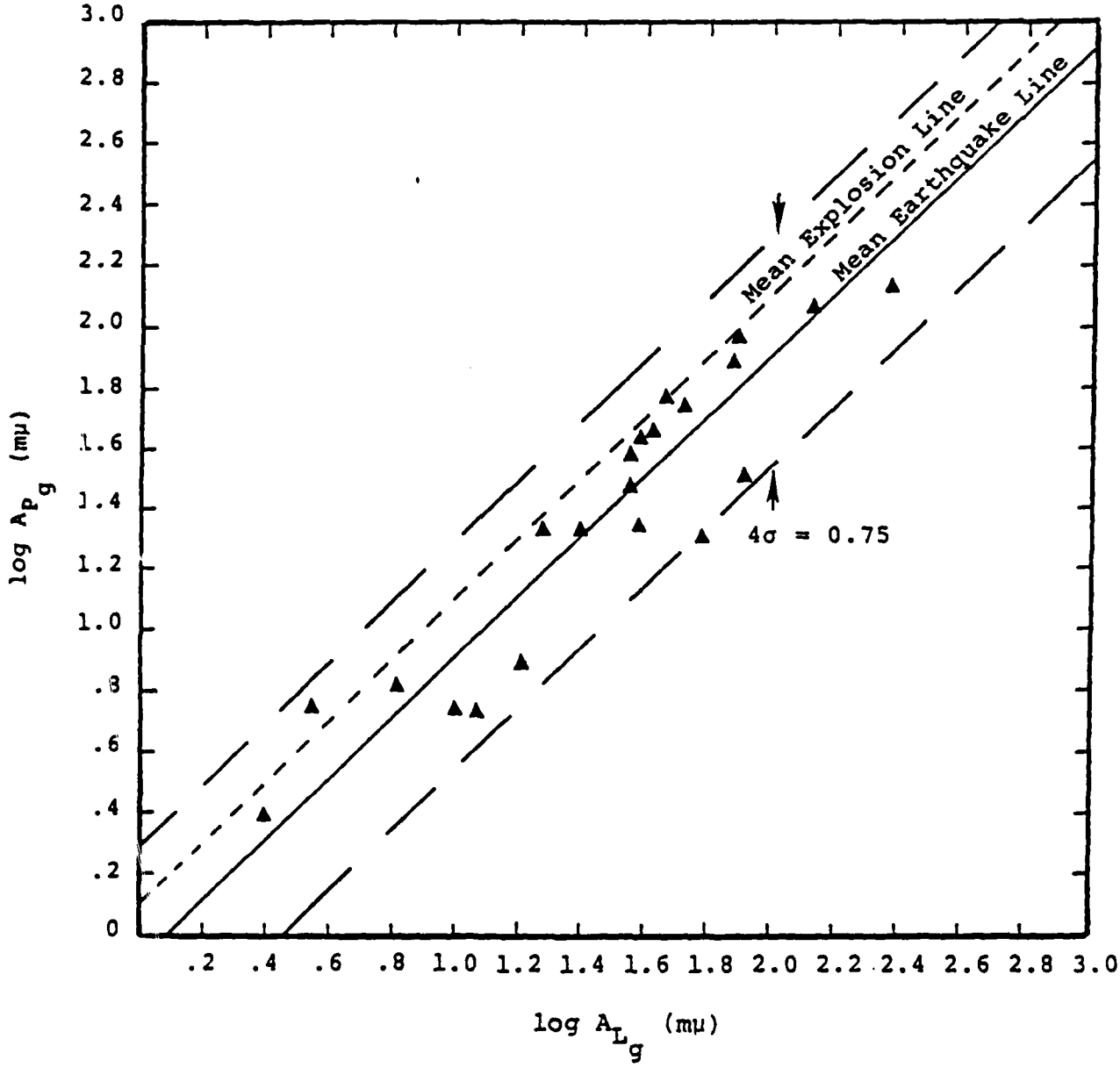

Figure 28. P_g/L_g amplitude data from NTS earthquakes recorded at Station TFO.

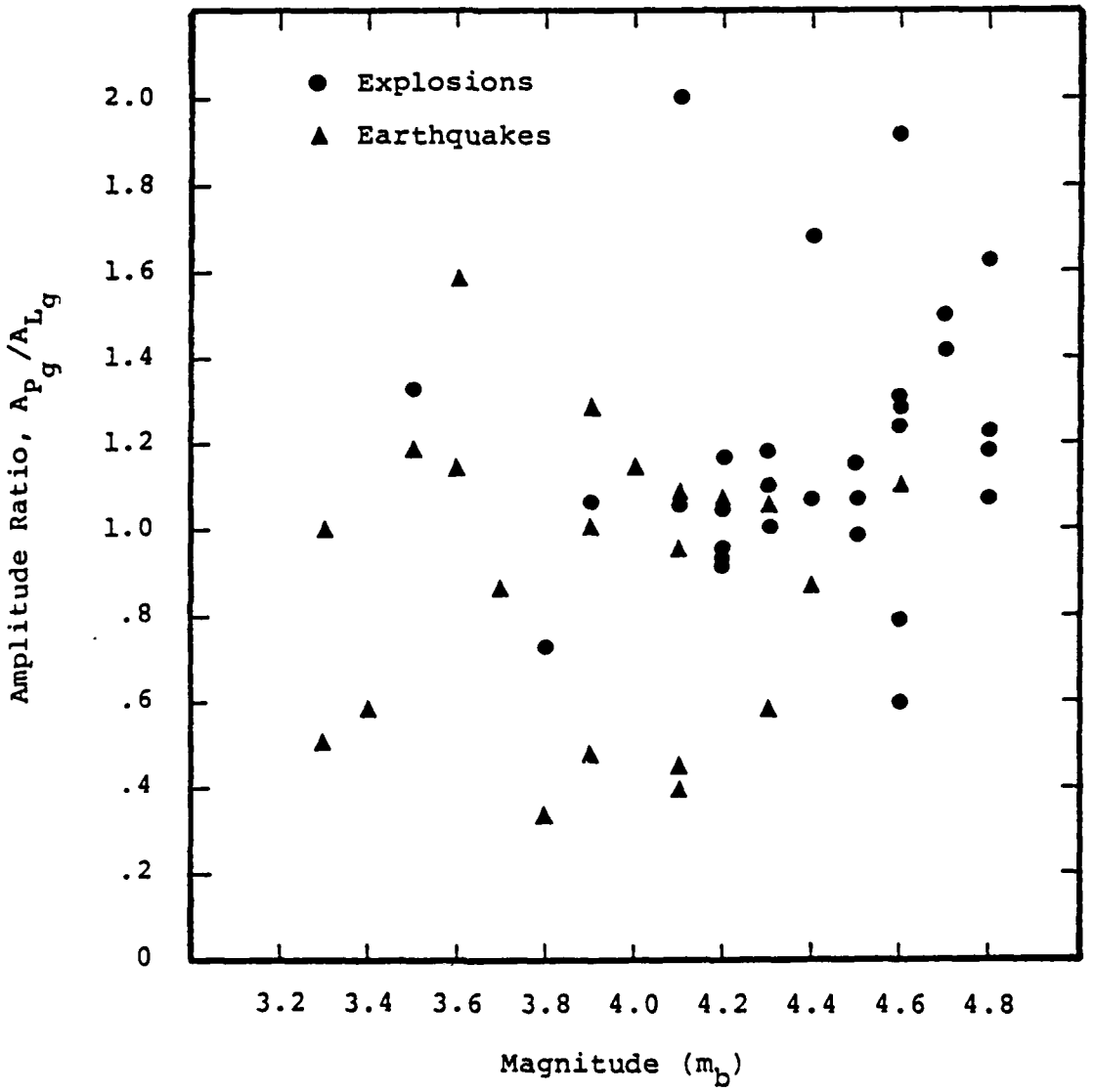

Figure 29. Comparison of NTS earthquake and explosion Pg/Lg amplitude ratios at Station TFO.

amplitude ratio (Bennett and Murphy, 1980). Thus, the evidence presented by this well controlled data set suggests that the L_g/P amplitude ratio may not be a very reliable discriminant. However, there are some preliminary indications that there may be some diagnostic differences in the spectral composition of the L_g phases associated with the two source types. This is illustrated in Figure 30 which shows a comparison of the dominant period of L_g as a function of m_b for the TFO sample of explosions and earthquakes. It can be seen that, for a given m_b, there is a tendency for the dominant period of the explosively generated L_g to be larger than that of the corresponding earthquake L_g. This is not the case for P_n, as is illustrated in Figure 31. Thus, although the L_g/P amplitude discriminant does not appear to be particularly robust, there is evidence that an L_g/P_n spectral discriminant may have good resolving power. More research will be required to adequately test and characterize this new discriminant.

4.3 M_s/m_b AT REGIONAL DISTANCES

Perhaps the most diagnostic discriminant for shallow focal depth events is the difference in surface wave excitation between earthquakes and explosions of the same body wave magnitude. Thus, it has been consistently observed (e.g. Liebermann and Pomeroy, 1969) that shallow earthquakes produce teleseismic surface wave amplitudes which are as much as an order of magnitude larger than those produced by explosions of the same body wave magnitude. The major problem associated with this discriminant is that the teleseismic detection threshold for M_s is significantly higher than that for m_b and, consequently, it cannot be applied to small events near the body wave magnitude detection threshold. Moreover, M_s at teleseismic distances is associated with surface waves with periods near 20 seconds and it is difficult to detect energy in such low frequency bands at regional distances. Therefore,

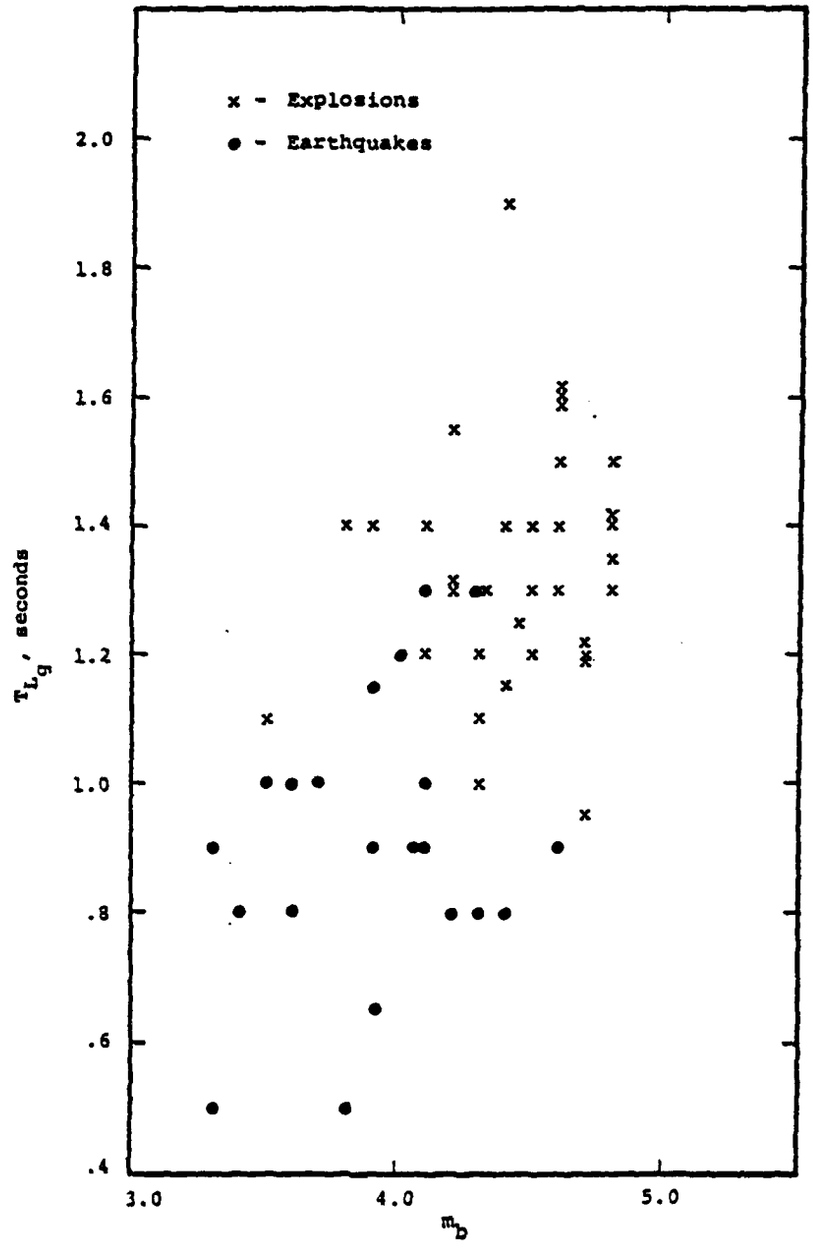

Figure 30. Comparison of dominant L_g periods for NTS earthquakes and explosions recorded at Station TFO.

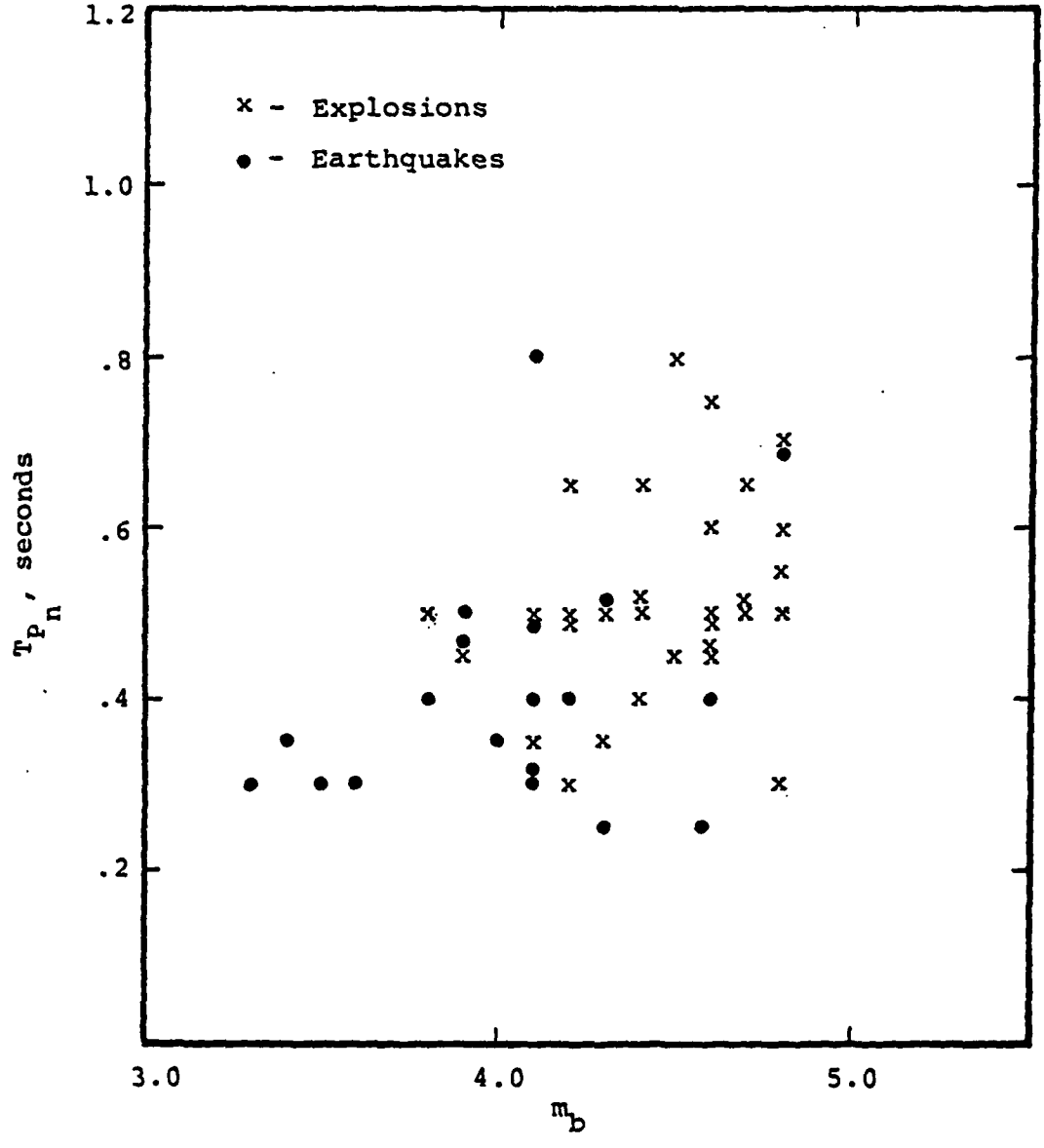

Figure 31. Comparison of dominant P_n periods for NTS earthquakes and explosions recorded at Station TFO.

it is not clear that the classical teleseismic M_s/m_b criterion can be directly applied to regional data. However, some attempts have been made to use shorter period surface waves in conjunction with regional P phase data to define a discriminant analogous to teleseismic M_s/m_b.

Peppin and McEvilly (1974) analyzed Rayleigh wave and P_n amplitude data from 56 NTS seismic events recorded at four broadband monitoring stations located at various azimuths at distances from NTS of between 230 and 500 km. These events included explosions, cavity collapses, explosion aftershocks and natural tectonic events, including some with magnitudes (M_L) as low as 3.0. The Rayleigh wave measurement was taken to be the amplitude at a period of 12 seconds as observed on a bandpass filtered version of the original broadband signal. The short period measurement was the maximum P_n amplitude, again read from a bandpass filtered version of the original broadband signal. For explosions, the dominant P_n frequencies were in the 2-4 Hz range, while the corresponding frequency bands characteristic of earthquakes and cavity collapses were 2-3 Hz and 0.75-1.50 Hz respectively. Figure 32 shows the Rayleigh amplitudes plotted versus the corresponding P_n amplitudes for the stations Elko and Kanab, located north and east of NTS respectively. Figure 33 presents a similar display for stations Landers and Mina, located south and west of NTS. It can be seen that the explosions are generally well separated from the earthquakes down to the smallest magnitudes measured. Moreover, although the separation is clearly better at Mina than at the other three stations, there is no indication that variations in focal mechanism are seriously affecting discrimination capability at any given station. Thus, it appears that this discriminant should be useful in a single station context. However, it should be noted that Peppin (1976), in a later study, found that when the maximum P_g spectral amplitude in the 0.8-1.0 Hz frequency band is plotted against the

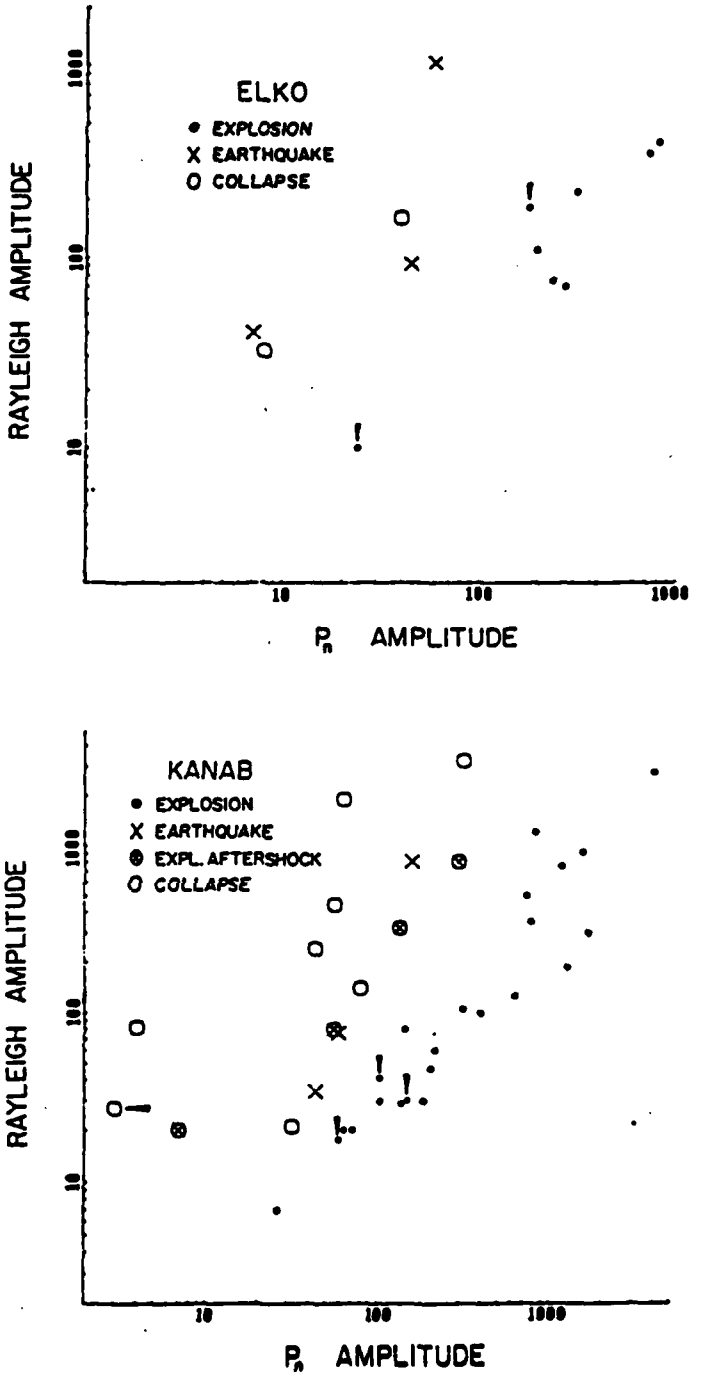

Figure 32. Rayleigh versus P_n amplitudes for NTS events recorded at Elko, Nevada and Kanab, Utah. Cuniforms denote upper limit readings (Peppin and McEvilly, 1974).

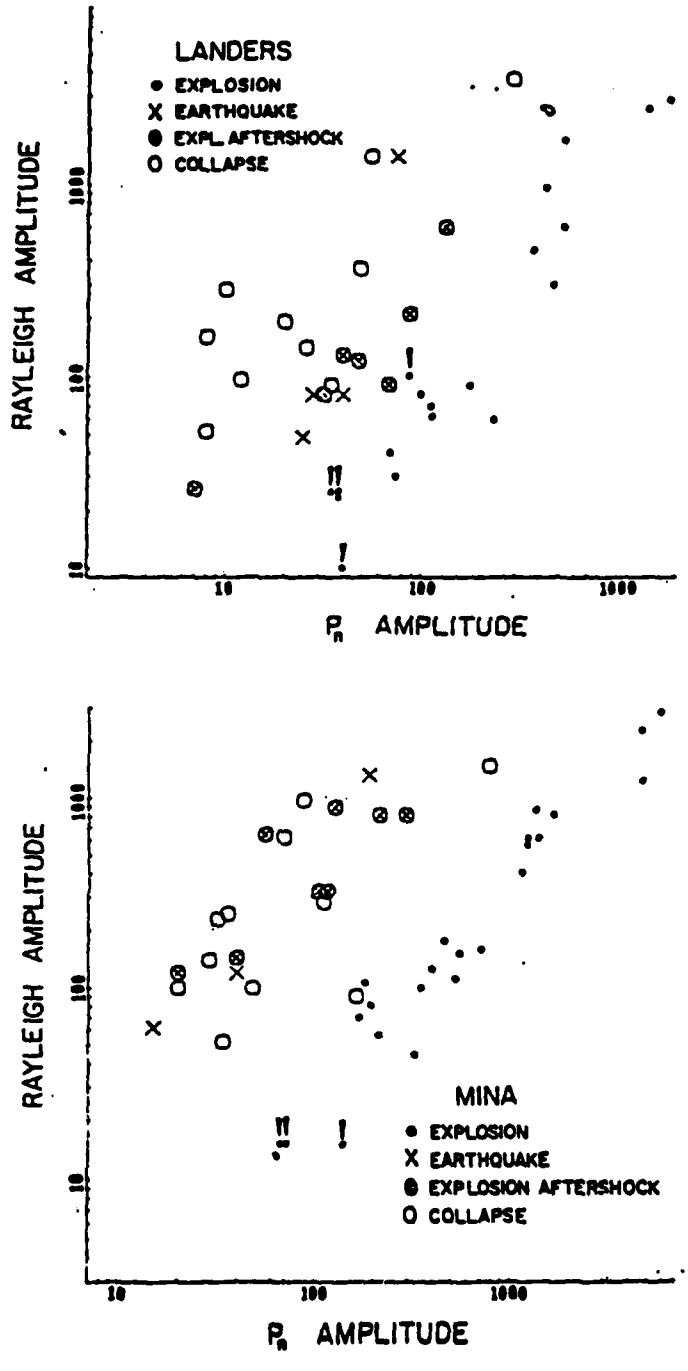

Figure 33. Rayleigh versus P_n amplitudes for NTS events recorded at Landers, California and Mina, Nevada. Cuniforms denote upper limit readings (Peppin and McEvilly, 1974).

corresponding 12 second Rayleigh wave amplitude level, the earthquake and explosion populations do not separate. The reason for this discrepancy between the results from P_g versus P_n is not yet known, although it may be associated with the dependence of P_g on focal depth (Peppin, 1976). In any case, the available evidence suggests that single station, regional P_n and Rayleigh wave data can be used in a manner analogous to teleseismic M_s/m_b data to provide a robust discriminant which will differentiate earthquakes from explosions.

4.4 SHORT-PERIOD P WAVE SPECTRAL DISCRIMINANTS

It was noted above that one of the fundamental limitations of body wave/surface wave type discriminants is that, in order to apply them, it is necessary that the long period surface waves be recorded at a reasonable signal-to-noise ratio, and this is often a problem for small events down near the detection threshold. Thus, in recent years, there have been numerous attempts to develop a spectral discriminant which can be applied to short-period P wave data alone (e.g. Bakun and Johnson, 1970; Savino and Archambeau, 1974). The most successful of these has been the MARS discrimination processor (Savino and Archambeau, 1974; Masso et al., 1979) which operates by comparing P wave magnitudes computed in a low and high frequency band. In this approach, the recorded seismic signal is passed through a series of specifically designed narrowband filters covering the frequency range over which the signal-to-noise ratio is adequate to permit the confident estimation of signal amplitude levels. Using these filter outputs, individual P wave arrivals are isolated and their spectral composition is determined. The amplitude levels in low and high frequency bands are then used to define frequency dependent body wave magnitude estimates, $m_b(f)$, which are compared for discrimination purposes. Figure 34 shows an example of the application of this procedure to

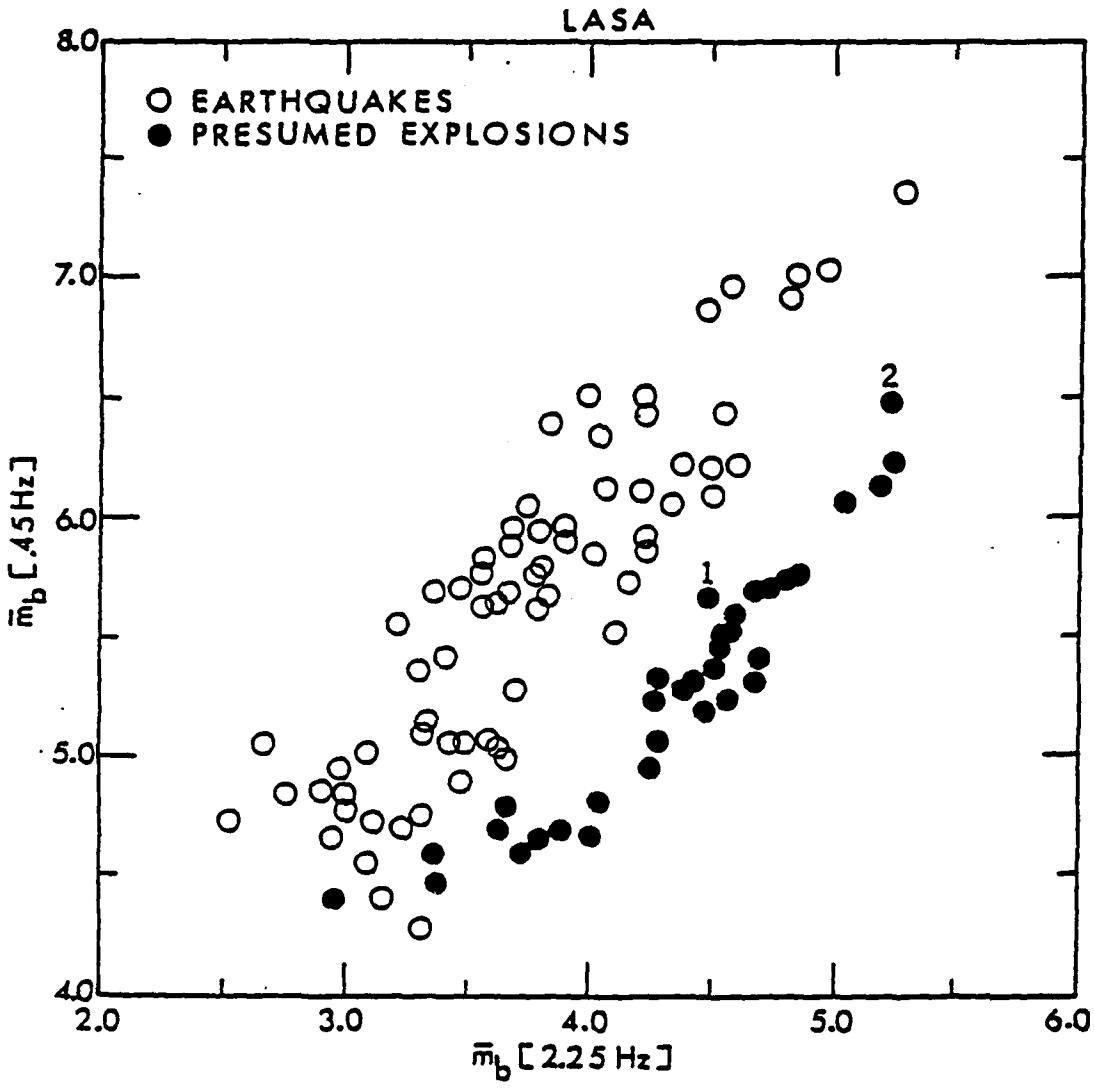

Figure 34. Comparison of P wave spectral magnitudes computed at 0.45 Hz and 2.25 Hz from a sample of Russian earthquakes and explosions recorded at the LASA seismic array in Montana.

teleseismic recordings of Russian explosions and earthquakes from the LASA seismic array in Montana (Masso et al., 1979). It can be seen that in this case, comparison of body wave magnitudes computed at 0.45 and 2.25 Hz results in almost complete separation of the earthquake and explosion populations. Moreover, experience gained during the recent AFTAC-sponsored teleseismic discrimination experiment has confirmed that this short-period P wave spectral discriminant can provide accurate source classifications for the majority of the events of interest.

The success of this discriminant against teleseismic data has provided the stimulus to derive an analogous capability for the analysis of regional data. Although this research is only just beginning, it is felt that the availability of broadband data from regional events should, in principle, permit even more confident discrimination in that magnitudes can be estimated at widely separated frequencies. Some preliminary support for this hypothesis is provided in Figure 35, which shows a comparison of low frequency (0.55 Hz) and high frequency (4.00 Hz) magnitude data for Russian explosions and earthquakes recorded at regional distances at station KAAO, Kabul, Afghanistan. It can be seen that the separation of the explosions and earthquakes at KAAO is even better than that obtained teleseismically (cf. Figure 34), presumably because of the greater separation in the available body wave magnitude frequency bands. Moreover, again there is no indication that variations in earthquake focal mechanism will seriously compromise the separation capability. Thus, these preliminary results suggest that regional P wave data can be used to define a short period spectral discriminant which should be applicable to single station data. This hypothesis is currently being tested against a larger sample of data.

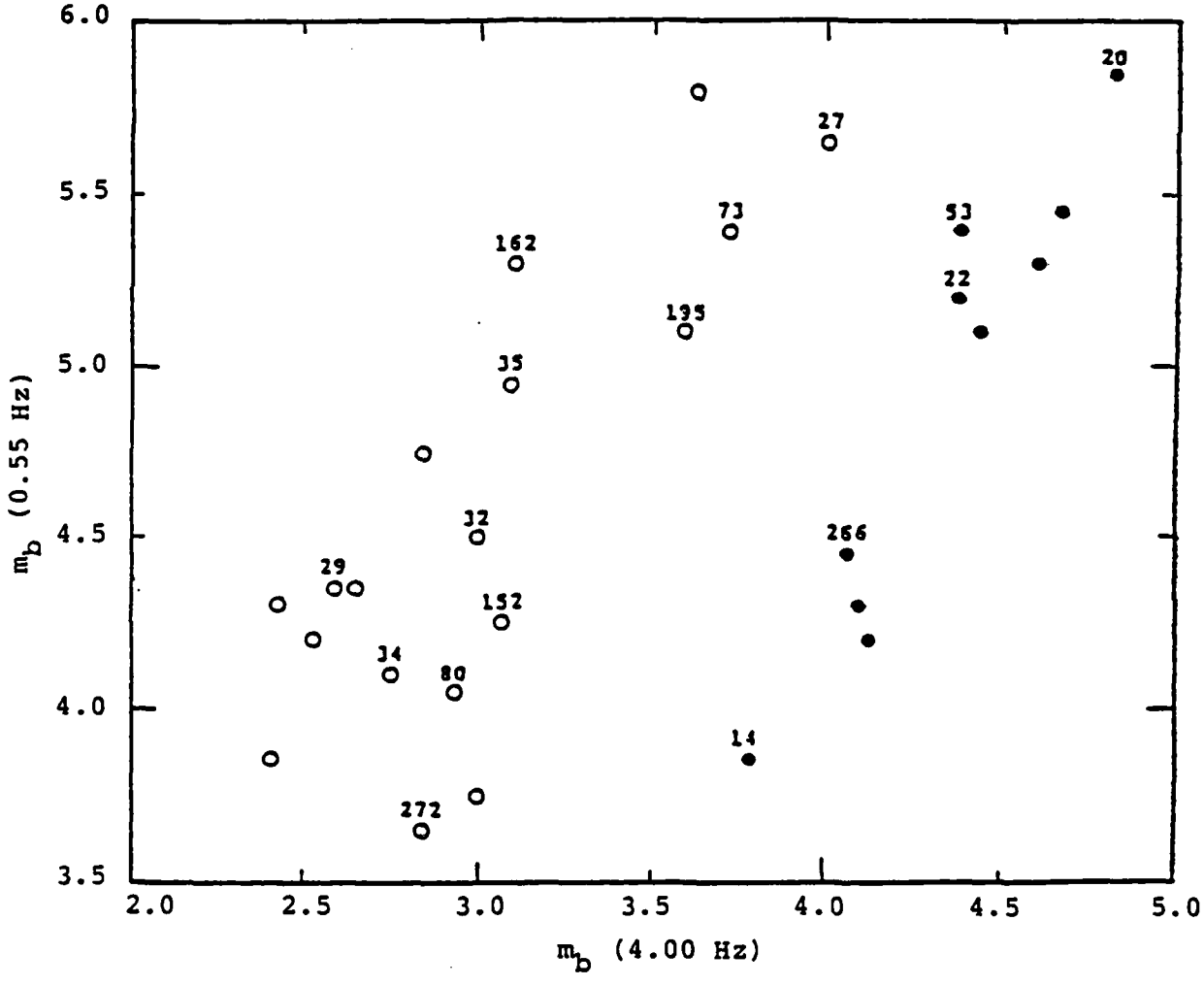

Figure 35. Comparison of regional P wave spectral magnitudes computed at 0.55 and 4.00 Hz from a sample of Russian earthquakes and explosions recorded at Station KAAO, Kabul, Afghanistan.

V. SUMMARY AND CONCLUSIONS

5.1 SUMMARY

The investigation summarized in this report has centered on an assessment of the various factors affecting the detection, location and identification capability of a single seismic station in the regional distance range. In particular, the present effort has encompassed an extension of previous analyses to include a consideration of the potential advantages associated with the analyses of the broadband seismic data which can be recorded in this distance range.

In Section II, a regional seismic detection model was described and applied to the frequency-dependent detectability of underground explosions in a variety of geologic environments. The components of the model include quantitative descriptions of the explosive seismic source functions, the propagation paths followed by the seismic energy between the source and receiver and the background seismic noise conditions at the recording site. This model was calibrated with respect to data recorded in the Eastern U.S. from the Salmon explosion and used to assess the dependence of the detection thresholds on the various model parameters. As a result of this analysis, it was demonstrated that P waves from contained explosions with yields as small as 1 kt should be detectable at ranges on the order of 1000 km or more over regional propagation paths similar to those characteristic of the Eastern U.S.

The location of seismic events using data recorded at only a single station was discussed in Section III where regional interphase arrival times were used to determine epicentral distance and three-component, particle motion data were used to constrain the azimuth of the source. With regard to the determination of epicentral distance, a variety of simulation experiments were conducted which indicated that accuracies on the order of 10 to 15 km should be attainable

using data from a calibrated regional station at which multiple phases are well recorded. Results of recent experiments on the determination of source azimuth from the polarization of P and L_g phases recorded at Eastern U.S. seismic stations were also summarized and used to infer that accuracies of better than 10 degrees should be attainable through particle motion analyses of regional phase data recorded at a single calibrated station.

Single station event discrimination capability was reviewed in Section IV with particular emphasis on the applicability of the L_g/P, M_s/m_b and short-period P wave spectral discriminants to the classification of regional seismic data. It was found that although questions remain concerning the general applicability of the simple L_g/P amplitude ratio discriminant, preliminary evidence suggests that regional versions of the M_s/m_b and short-period P wave spectral discriminants should provide good event separation, in most cases, when applied to single station data.

5.2 CONCLUSIONS

The analyses summarized above support the following conclusions concerning the seismic detection of fully coupled underground explosions at regional distances.

1. The seismic coupling of explosions in wet tuff/rhyolite, granite and shale source environments are expected to be quite similar, while explosions in salt are expected to couple significantly better and explosions in dry alluvium/tuff significantly less well than those in the other three media. The predicted difference in coupling between salt and dry alluvium/tuff is as much as a factor of ten within the frequency range of interest with respect to regional detection.

2. Even at regional distances, the frequency components which define the limits of detectability for explosions with yields of about 1 kt lie in the 2-3 Hz range. Thus, the availability of broadband data is of less significance with regard to the detection of fully coupled explosions than in the previously considered detection of decoupled explosions (Murphy, 1980).

3. For regional propagation paths similar to those of the Eastern U.S., even 1 kt explosions in low coupling media such as dry alluvium/tuff should be detectable at quiet sites at ranges exceeding 2000 km, at least over a limited frequency band. The most important factor influencing detectability is the frequency-dependent, seismic wave attenuation associated with the regional propagation paths of the phases of interest.

With regard to the location of seismic events using data recorded at a single regional station, results of studies conducted to date lead to the following conclusions.

1. The results of preliminary studies suggest that epicentral distance can generally be estimated to within 10 to 15 km using data recorded at a calibrated station at which multiple regional phases are well recorded. At stations where the phases of interest are less distinct, and only times of occurrence of maximum phase amplitude can be reliably determined, the uncertainty in the single-station epicentral distance estimate may be expected to be at least twice this large.

2. Available evidence suggests that somewhat better accuracy in the epicentral distance estimate may be attainable using data from a station located in close proximity (i.e. at a range on the order of 100 km) to an area of special interest (e.g. salt domes). Simulation analyses suggest that routine processing of the recorded data may provide accuracies of better than 4 km in such cases.

3. Available evidence suggests that particle motion processing of three component regional phase data recorded at a single calibrated station should permit a determination of source azimuth with an accuracy of better than 10 degrees. At a range of 1000 km an azimuth error of 10 degrees translates into a location error of about 175 km, which is large with respect to the above-quoted uncertainty in single station estimates of epicentral distance. Thus, azimuth estimation is generally the greatest source of uncertainty in single station event location.

Finally, with regard to the classification of seismic events using single station data, results of studies conducted to date lead to the following conclusions.

1. Extensive research has only recently been initiated on the development of a regional discrimination capability and many of the proposed discriminants have not yet been adequately tested. At the present time, the most promising regional discriminants appear to be those based on ratios of

regional phases such as L_g/P, and regional versions of the teleseismic M_s/m_b and short-period P wave spectral discriminants.

2. Questions remain concerning the general applicability of the simple L_g/P amplitude ratio discriminant. However, there are some preliminary indications that an L_g/P spectral ratio discriminant may provide more consistent event separation.

3. A regional version of M_s/m_b based on the ratio of the P_n amplitude to the amplitude of the Rayleigh wave at periods near 12 seconds provides good separation between Nevada Test Site earthquakes and explosions. At present, there are no indications that variations in the focal mechanisms of the earthquakes seriously degrade this separation and, thus, this discriminant should be useful in a single station context for those cases in which the Rayleigh wave signal can be detected.

4. Preliminary spectral analyses of regional P wave data recorded from Russian explosions and earthquakes suggest that the single station short-period P wave spectral discriminant may be even more effective against such broadband data than it is against teleseismic data from the same events.

REFERENCES

Bakun, W. H. and L. R. Johnson, 1970, "Short Period Spectral Discriminants for Explosions," Geophys. J. R. Astr. Soc., 22, p. 139.

Bennett, T. J. and J. R. Murphy, 1980, "A Study of the Relative Excitation of Regional Phases for Use in Event Discrimination" Paper Presented at the Annual Meeting of the Eastern Section of the Seismological Society of America, October.

Blandford, R. and P. Klouda, 1980, "Magnitude-Yield Results at Tonto Forest Observatory," in Studies of Seismic Wave Characteristics at Regional Distances, Teledyne Geotech Final Report, AL-80-1, Air Force Office of Scientific Research Contract F49620-79-C-0031.

Blandford, R. and R. Hartenberger, 1978, "Regional Discrimination Between Earthquakes and Explosions (Abstract)," EOS, Trans. Am. Geophys. Union, 59, p. 1140.

Bollinger, G. A., 1970, "Travel-Time Study of Six Central Appalachian Earthquakes," Bull. Seismol. Soc. Am., 60, p. 629.

Evernden, J. F., 1976, "Study of Seismological Evasion. Part II. Evaluation of Evasion Possibilities Using Normal Microseismic Noise," Bull. Seismol. Soc. Am., 66, p. 281.

Gupta, I. N. and J. A. Burnetti, 1980, "An Investigation of Discriminants For Events in Western USSR Based on Regional Phases at a Single Station," in Studies of Seismic Wave Characteristics at Regional Distances, Teledyne Geotech Final Report, AL-80-1, Air Force Office of Scientific Research Contract F49620-79-C-0031.

Jordan, J. N. W. V. Mickey, Wayne Helterbran and D. M. Clark, 1966, "Travel Times and Amplitudes from the Salmon Explosion," J. Geophys. Res., 71, p. 3469.

Liebermann, R. C. and P. W. Pomeroy, 1969, "Relative Excitation of Surface Waves by Earthquakes and Underground Explosions," J. Geophys. Res., 74, p. 1575.

Masso, J. F., C. B. Archambeau and J. M. Savino, 1979, "Implementation, Testing and Specification of a Seismic Event Detection and Discrimination System," SSS-R-79-3963, Final Report to U.S. Arms Control and Disarmament Agency Under Contract AC8-MC106.

Mueller, R. A. and J. R. Murphy, 1971, "Seismic Characteristics of Underground Nuclear Detonations Part I. Seismic Spectrum Scaling," Bull. Seismol. Soc. Am., 61, p. 1675.

Murphy, J. R., 1977, "Seismic Source Functions and Magnitude Determinations for Underground Nuclear Detonations," Bull. Seismol. Soc. Am., 67, p. 135.

Murphy, J. R., 1978, "Seismic Coupling and Magnitude/Yield Relations for Underground Nuclear Detonations in Salt, Granite, Tuff/Rhyolite and Shale Emplacement Media (U)," Computer Sciences Corporation Technical Report submitted to VSC/ARPA, CSC-TR-78-0004, October (Secret).

Murphy, J. R., 1980, "An Evaluation of the Factors Influencing the Seismic Detection of Decoupled Explosions at Regional Distances," SSS-R-80-4579, Final Report to U.S. Arms Control and Disarmament Agency Under Contract AC9MC107.

Murphy, J. R., 1981, "Magnitude/Yield Relations For Explosions and Their Dependence on Source Medium and Depth of Burial," Systems, Science and Software Technical Report submitted to VSC/ARPA, SSS-CR-81-4886, March (Secret).

Peppin, W. A. and T. V. McEvilly, 1974, "Discrimination Among Small Magnitude Events on Nevada Test Site," Geophys. J. R. Astr. Soc., 37, p. 227.

Peppin, W. A., 1976, "P Wave Spectra of Nevada Test Site Events at Near and Very Near Distances: Implications For a Near-Regional Body Wave-Surface Wave Discriminant," Bull. Seismol. Soc. Am., 66, p. 803.

Pomeroy, P. W., 1978a, "An Investigation of Seismic Wave Propagation in Eastern North America," Rondout Associates, Semi-Annual Technical Report Under Contract F49620-78-C-0043.

Pomeroy, P. W., 1978b, "An Investigation of Seismic Wave Propagation in Western U.S.S.R.," Semi-Annual Technical Report No. 2 Under Contract F49620-78-C-0043.

Savino, J. M. and C. B. Archambeau, 1974, "Discrimination of Earthquakes from Single and Multiple Explosions Using Spectrally Defined Event Magnitudes," Trans. Amer. Geophys. Union, EOS (Abstract), 56, p. 1148.

Smart, E., 1978, "A Three-Component, Single-Station, Maximum-Likelihood Surface Wave Processor," Teledyne Geotech Technical Report submitted to VSC/ARPA, SDAC-TR-77-14.

Smart, E. and H. Sproules, 1981, "Regional Phase Processors," Teledyne Geotech Technical Report submitted to VSC/ARPA, SDAC-TR-81-1.

Stauder, W., R. Herrmann, S. Singh, R. Perry, R. Dwyer, M. Meremonte, V. Masih, L. Himes, E. Haug, S. Morrissey, L. Hausman and M. Whittington, 1981, "Central Mississippi Valley Earthquake Bulletin, Quarterly Bulletin No. 26, Fourth Quarter 1980", Department of Earth and Atmospheric Sciences, St. Louis University.

Willis, D. E., J. DeNoyer and J. T. Wilson, 1963, "Differentiation of Earthquakes and Underground Nuclear Explosions on the Basis of Amplitude Characteristics", Bull. Seismol. Soc. Am., 53, p. 979.